UNIVERSITY OF SOUTHERN QUEENSLAND

FACULTY OF HEALTH, ENGINEERING AND SCIENCES

SOIL COMPACTION DEPENDENCE ON SUB-FIELD SPATIAL SOIL CONSTRAINT VARIABILITY

A dissertation written by,

Danny O'Connor

In line with the requirements included in courses ENG4111 and ENG4112

Towards the degree of,

Bachelor of Engineering (Honours)

(Majoring in Agriculture)

Submitted October 2022

LIMITATIONS OF USE

CERTIFICATION OF DISSERTATION

I certify that the ideas, designs and experimental work, results, analyses and conclusions set out in this dissertation are entirely my own effort, except where otherwise indicated and acknowledged. I further certify that the work is original and has not been previously submitted for assessment in any other course or institution, except where specifically stated.

Danny O’Connor

Student Number: [redacted]

Signature: [redacted]

Date: 13/10/2022

PROJECT TITLE

Soil compaction dependence on sub-field spatial soil constraint variability

ABSTRACT

Soil constraints are known to vary spatially at the sub-field level, both across area and with depth. The impact of these, varying with time, are largely driven by moisture content status. Soil compaction is a soil constraint that is difficult to determine due to the requirement of a natural benchmark condition (soil density prior to any traffic or operation) or proximal benchmark condition (spatially natural soil proxy), both of which are almost impossible to obtain for most models. For this reason, the focus on soil compaction has been on vulnerability and susceptibility of soils throughout the landscape. However, as on-farm management moves towards a finer scale of land management unit (LMU), approaching machine frontage resolution (e.g., 12x12m LMU based upon a 12 m operational frontage system), industry discussion has shifted to the sub-field variability of soil compaction vulnerability and susceptibility, an influential factor which remains unknown. It was suspected that the magnitude of stress imparted on the soil by modern harvesting machines would be far greater than the sub-field variability of vulnerability and susceptibility, meaning that alleviation of compaction incidence should be the first step for best management practice. This study was conducted to provide laboratory-based evidence for stress state impact based upon sub-field soil type and constraint diagnosis, at four fields, for a range of moisture contents. Outcomes from the investigation suggest no direct relationships can be drawn between soil pedological factors and constraints. This comes with the observation of significant variance in compaction parameters at the subfield scale, at a rage of sites. In spite of this, the degree of compactness as measured from the samples indicate crop growth will be restricted under these conditions. Inferring the key message being the overriding effect of stress on compaction and hydraulic reduction despite sub-field variability.

ACKNOWLEDGEMENTS

First and foremost, I would like to thank Professor John McLean Bennet for his guidance and support in initiation and throughout this project. John's generosity and expertise has instituted my interest within the field of soil science and is accountable for the knowledge I have gained through the duration of this project.

Also, I would like to achnowledge and register my appreciation towards my official project supervisor, Associate Professor Guangnan Chen who was required to step into this role at short notice.

A special thank you deserves to go to Stirling Roberton and Ned Skehan for their support throughout this project, particularly for their assistance in completing sub-field soil diagnosis.

I would like to thank David West for his assistance and compassion in both the field and laboratory work throughout this project. Furthermore, this thanks should be extended to the CRDC for providing the funding to collect the required field samples.

Thanks to Craig Lobsey, Wayne Crowell, Aram Ali and Piumika Ariyadasa for their contributions to the engineering aspects of this project, specifically throughout the extensive uniaxial compression testing, which was made bearable thanks to their efforts.

Also, to the University of Southern Queensland and Centre for Agricultural Engineering (CAE) for granting me the opportunity to undertake this thesis, providing access to the required facilities and allowing me to make a contribution to the research community.

Finally, I would like to express my appriecation to all of my close friends and family for their encouragement and support throughout this project.

LIST OF FIGURES

Figure 2.1 Stresses in a volume under a point of applied load (Défossez & Richard, 2002) 14
Figure 2.2 Stresses acting on a volume of soil considering pressure distribution by a contact area between tyre and soil according to (Söhne, 1953), (Défossez & Richard, 2002). 15
Figure 2.3 Plot of reduction in Ksat in an arable subsoil caused by an increase in machinery weight (BLUE) based on relative bulk density (RED) as estimated by the pedo-transfer function (Keller et al., 2019). 16
Figure 2.4 Relationship between soil water content and bulk density for analysis of compaction (Ishaq et al., 2001). 22
Figure 3.1 Geographic location of all 16 experimental sites analysed in the USQ1903 CRDC project with the RED outline detailing the sites selected from this project and changes in sampling point colour indicating varying constraint values of each point. 27
Figure 3.2 Experimental sites (A) DALBY- Shawn Fresser Field 3, (B) DALBY- Steve McVeigh Field 4, (C) TALWOOD- Ben Turner Field 7, and (D) TALWOOD- Tom Seerey Field 8, detailing the 20 sampling locations from the USQ1903 CRDC project, with red outline indicating the locations selected for this project. Changes in sampling point colour indicate the describing constraint value as seen in the legend below. 28
Figure 3.3 (A) Handheld Trimble GPS unit and receiver alongside sample collection apparatus, (B) soil pit from which sample was collected (volume approx. 15000 $cm3$). Both images are taken at location: TALWOOD- Ben Turner Field 7. 29
Figure 3.4 Procedure for sample analysis (A) labelled samples in soil oven, drying to 40 degrees celcius, (B) Casagrande apparatus used to determine sample liquid limit, (C) crumbling samples rolled to 3mm diameter, indicating sample plastic limit, (D) plot of moisture content versus the number of blows observed in the Casagrande procedure used to determine sample liquid limit. 30
Figure 3.5 Sample preparation procedure (A) soil grinder set to an opening of 10mm to break down large aggregates/ clods, (B) 6.7mm sieve used to filter trash and stones from field samples, (C) apparatus used for uniaxial compression sample preparation in PVC cylinder, (D) samples moistened, sealed and left to equilibrate for 24 hours before uniaxial compression. 32
Figure 3.6 Uniaxial compression procedure (A) 50 kN MATEST CBR Tester screw type press, (B) 6mm rubber disk bonded to 10mm steel spherical plate used to compress soil, (C) steel proctor mould and 90mm bore casing used to support sample in compression, (D) catmanEasy V4.1.1 program used to record test outputs, load and deflection. 34
Figure 3.7 Diagram of mini disk infiltrometer used to measure infiltration rates in soil. 35
Figure 3.8 Apparatus used to measure soil infiltration rates (A) samples prepped for infiltration testing with a thin layer of silica sand, (B) nine AMDIs in place and recording infiltration rates on compressed samples. 36
Figure 3.9 Plots of cumulative infiltration with time (A) example of a test requiring data cleaning (break in hydraulic contact occurs at t = 3100s), (B) example of a test which does not require data cleaning. 37
Figure 4.1 Compression curves from uniaxial compression tests completed for the following: (A) SAMPLE 3_3, (B) SAMPLE 3_9, (C) SAMPLE 3_12, (D) SAMPLE 3_18, (E) SAMPLE 4_6, (F) SAMPLE 4_9, (G) SAMPLE 4_15, (H) SAMPLE 4_16, (I) SAMPLE 7_6, (J) SAMPLE 7_7, (J) SAMPLE 7_18, (K) SAMPLE 7_20, (L) SAMPLE 8_1, (M) SAMPLE 8_3, (N) SAMPLE 8_3, (O) SAMPLE 8_7, (P) SAMPLE 8_9 detailing the change in bulk density as moisture content increases for each of the 3 stress states. 44
Figure 4.2 Hydraulic conductivity plots (A) samples from field 3, stress state: 50 kPa, (B) samples from field 3, stress state: 100 kPa, (C) samples from field 3, stress state: 350 kPa, (D) samples from

field 4, stress state: 50 kPa, (E) samples from field 4, stress state: 100 kPa, (F) samples from field 4, stress state: 350 kPa, (G) samples from field 7, stress state: 50 kPa, (H) samples from field 7, stress state: 100 kPa, (I) samples from field 7, stress state: 350 kPa, (J) samples from field 8, stress state: 50 kPa, (K) samples from field 8, stress state: 100 kPa, (L) samples from field 8, stress state: 350 kPa detailing the near saturated hydraulic conductivity of compressed samples at the 3 selected moisture contents. 46
Figure 4.3 Experimental sites (A) DALBY- Steve McVeigh Field 3, (B) DALBY- Shawn Fresser Field 4, (C) TALWOOD- Ben Turner Field 7, and (D) TALWOOD- Tom Seerey Field 8 with the red points detailing the relative location of each selected monitoring point, in each field. The text conveys the results found for plastic limit and hydraulic conductivity of a soil sample collected from that point. The value for hydraulic conductivity is measured after simulated machine induced compaction (stress state of 350 kPa) at each soil's specific plastic limit. 49
Figure 4.4 Analysis of sub- field variance between mean bulk densities after compaction at 3 specific moisture contents for each stress state (A) ANOVA at DALBY- Steve McVeigh Field 3, (B) ANOVA at DALBY- Shawn Fresser Field 4, (C) ANOVA at TALWOOD- Ben Turner Field 7, and (D) ANOVA at TALWOOD- Tom Seerey Field 8 50
Figure 4.5 Analysis of sub- field variance between mean hydraulic conductivities after compaction at 3 specific moisture contents for each stress state (A) ANOVA at DALBY- Steve McVeigh Field 3, (B) ANOVA at DALBY- Shawn Fresser Field 4, (C) ANOVA at TALWOOD- Ben Turner Field 7, and (D) ANOVA at TALWOOD- Tom Seerey Field 8. Where absent data points are substituted with local means (Shaw & Mitchell-Olds, 1993) 51
Figure 4.6 Analysis of variance in degree of compaction between fields (A) ANOVA between mean bulk densities after compaction at each soil's plastic limit for each stress state, (B) ANOVA between mean hydraulic conductivities after compaction at each soil's plastic limit for each stress state, where absent data points are substituted with local means (Shaw & Mitchell-Olds, 1993). 52
Figure 4.7 Plot comparing applied load versus sample deflection produced from the uniaxial compression test for SAMPLE: 4_15, moistened to the soils specific plastic limit and load applied to simulate a surface stress state of 350 kPa. 53

LIST OF TABLES

Table 3.1 The three target gravimetric moisture contents, assumed for each sample before uniaxial compression testing. 31
Table 3.2 Pressures required to simulate target stress states and corresponding loads 33
Table 4.1 Soil properties from monitoring points at site 3. 39
Table 4.2 Soil properties from monitoring points at site 4. 40
Table 4.3 Soil properties from monitoring points at site 7. 40
Table 4.4 Soil properties from monitoring points at site 8. 40
Table 4.5 Sensitivity analysis on sample deflection with regards to applied load. 53

CONTENTS

Limitations of Use 1
Certification of Dissertation 2
Project Title 3
Abstract 3
Acknowledgements 4
List of Figures 5
List of Tables 7
1. Introduction 10
1.1 Background 10
1.2 Aim 11
1.3 Objectives 11
1.4 Dissertation Overview 12
1.4.1 Literature Review 12
1.4.2 Methodology 12
1.4.3 Results 12
1.4.4 Discussion 12
1.4.5 Conclusion 12
2. Literature Review 13
2.1 Introduction 13
2.2 Effects of Machine Stress on Soil Mechanics 13
2.2.1 Stress in Soil 13
2.2.2 Hydraulic Properties 15
2.3 Agronomic Effects and Extent of Compaction 16
2.4 Off-Site Impact and Mitigation Techniques 18
2.4.1 Australian Cotton 18
2.4.2 Managing Compaction 18
2.5 Spatial Dependence of Soil Compaction 19
2.5.1 Sub-field Constraint Variability 19
2.5.2 Spatial Variance of Soil Compaction 20
2.5.3 Spatial Mapping of Soil Compaction 20
2.6 Relations Between Load, Change in Density and Soil Texture 22
2.7 Uniaxial Compression Testing 23
2.8 Hydraulic Conductivity 23
2.9 Soil Stress State Modelling 24

2.10 Thesis Rationale 25
3. Methodology 26
3.1 Aims and Objectives 26
3.2 Procedure 26
3.2.1 Site selection and sub-field diagnostics 26
3.2.2 Monitoring point identification and sample collection 27
3.2.3 Uniaxial compression testing 29
3.2.4 Unsaturated Hydraulic Conductivity 34
3.3 Health, Safety and Ethics Clearance 38
4. Results 39
4.1 Soil Properties 39
4.2 Uniaxial Compression 41
4.3 Soil Hydraulic Properties 44
4.4 Spatial Variance 47
4.5 Statistical Analysis 50
4.5.1 Analysis of Variance 50
4.5.2 Outliers 52
4.5.3 Sensitivity Analysis 52
5. Discussion 54
5.1 Factors Contributing to Compaction Risk 54
5.2 Consequences of Compaction Extent 55
5.3 Considerations for Further Work 55
6. Conclusion 57
7. References 58
8. Appendices 63
8.1 Appendix A 63
8.2 Appendix B 64

1. Introduction

1.1 Background

Soil compaction can be defined as the reduction of pore space within a subject soil. This requires an applied load of a magnitude which exceeds the precompression strength of the soil (Chancellor et al., 1962) hence, increasing the soil's bulk density. This process may occur naturally; rain, hail, fluctuations in soil moisture content, or enhanced by an external force, agricultural machinery or livestock traffic. Compaction results in reduction of soil aeration, water infiltration, and hydraulic conductivity, (Berisso et al., 2012; Chyba et al., 2014). Similarly, it is considered to be a primary stimulus for the processes of physical soil degradation via erosion and the removal of soil organic carbon (Kadlec et al., 2012). Laboratory studies suggest the severity of these consequences is increased as dry soil approaches field capacity, as precompression strength decreases proportionally, (Hamza et al., 2011). This investigation looks to analyse the extent and effects of wheeled machinery traffic in order to resonate the significance of unsustainable farming management.

It is recognised that the decline in soil quality is one of the main threats faced by presented to Australian cotton growers (Antille et al., 2016). Approximately 75% of Australia's cotton is grown in Vertosol dominant regions, extending from Central Queensland to Southern parts of New South Wales. Although cotton traditionally performs well in this soil type, the majority of crops are irrigated to maintain the conservative required soil moisture range between plant available water stress, and excess or waterlogging (Daniells et al., 1996; Virmani et al., 1982). As Vertosols are partially defined by high clay contents, the associated minerals infer the characteristic shrink and swell properties with fluctuations in moisture content. In turn, these properties influence soil structural development and re-development, (Chinn & Pillai, 2008; Pillai & McGarry, 1999). Vertosols are thus particularly susceptible to physical degradation with improper management. Hence, a primary focus in the recent shift to conservative and sustainable agricultural practices has been minimising soil compaction. More specifically, reducing the mechanical stress applied to sub-field soil profiles by agricultural machinery wheels. A number of studies, (Barik et al., 2014) have looked at the prolonged effects of more traditional farming procedures, (heavy tillage rates and implements, large harvesters). Most of which have identified obvious correlations between the rate of mechanical disturbance or compaction and soil degradation in terms of physical soil properties including, aggregate stability (AS), bulk density (BD), total porosity (TP) and volumetric moisture content (VMC). With Australia's agricultural equipment industry worth roughly $3.71b (Kingsley et al., 2021) it is important that a comprehensive understanding of the implications inflicted by these machines is reached amongst the community. Furthermore, a reduction in saturated hydraulic conductivity is experienced in compacted soil, compromising the field water infiltration potential and initiating the increased effects of water erosion. Crops also endure high resistance in root growth, nutrient and water uptake in compacted soils, decreasing both growth and overall yields, further encouraging this loss in productivity.

1.2 Aim

Thorough investigation of the topic background reveals a of knowledge gap in industry-based literature. The abundance of yield mapping and remote sensing imagery available to most farmers has been catalytic to the widespread recognition of spatial variability and the in-field factors limiting yields. This has propagated a profusion of mitigation procedures predominantly focussing on standardising plant nutrient availability, (Castrignano et al., 2002) with little concentration on the soil physical property variability. Hence this project will particularly be conducted to quantify soil compaction extent as affected by spatial variability at the sub-field scale with respect to soil type and soil constraint changes. It is perceived in the agricultural community that ameliorating the spatial occurrence of varying soil constraints should be the primary focus for best soil management. However, it is suspected that the magnitude of mechanical stress imparted by machine traffic outweighs the effect of spatial variability of soil constraints within a soil type at the sub-field level. This means we expect that there will not be any significant variability in soil compaction impact for a given moisture content spatially within a given soil type. Which would suggest that we should focus predominantly on reducing compaction severity by discounting the mechanical stresses being applied rather than considering the particular soil constraints.

1.3 Objectives

Extending from the aim above are the following series of objectives that need to be met in order to test the hypothesis thoroughly.

- Select a minimum of four sites (one field at each site)
- Spatially diagnose the soil type and soil constraint variability at the sub-field scale
- Using pedometric techniques, select representative monitoring points within the field from which to sample soil for compaction experimentation
- Using a uniaxial compression test, determine the change in density of the soil at a range of moisture contents and stress states for each monitoring location
- From the compressed sample, determine the hydraulic reduction with compaction severity
- Using the soil type and constraint diagnosis, investigate the interaction between constraints, depth, stress state and moisture content on the reduction in soil pore geometry as inferred from saturated hydraulic conductivity

The above tasks will provide a quantitative measure of the soil compaction extent as affected by spatial variability at the sub-field scale with respect to soil type and soil constraint changes for a variety of sites. Ultimately providing an outcome to be considered by land holders for future management practices.

1.4 Dissertation Overview

1.4.1 Literature Review

This section provides an analysis of the literature examining the significance of soil compaction experienced in the Australian Cotton industry and the parameters involved with this phenomenon. In addition to this, a review is made on a variety of soil properties and experimental procedures which test these, particularly aspects which are relevant to compaction.

1.4.2 Methodology

Here, the procedures conducted to obtain results required to address the project objectives are outlined in this section. More specifically, it includes a thorough explanation of the soil sampling process and the techniques implemented to achieve an informative outcome.

1.4.3 Results

This section presents the results derived from the study in an array of tables, plots and figures. A brief analysis of the findings is conducted, alluding to the final recommendations.

1.4.4 Discussion

This section highlights the relevance of the study and further conveys suggested areas of industry applicability. Encouraged management strategies derived from the results of this study are expressed, with the potential benefits and similarly, expected consequences of mismanagement defined.

1.4.5 Conclusion

This final section outlines the major outcomes of the study draws conclusions from the most critical results. Furthermore, the primary motives of the project are addressed with regards to relevant findings.

2. LITERATURE REVIEW

2.1 INTRODUCTION

Literature analysed in this review will compare the magnitude of machine stress and the spatial variability of underlying soil constraints. There is an industry perception that the spatial occurrence of soil constraints, (properties which inhibit crop growth) outweighs the impact of soil compaction. This has led to a focus on alleviating these soil constraints before moving to true controlled traffic farming (CTF). It can be argued that this is wasted effort as the overriding limitation is compaction given the magnitude of force and extent of homogenous impact. Hence, the review is conducted to ascertain the effect of equivalent machine stress on soils of different geographical and pedological nature. The review will focus on how machine stress affects soil mechanics, the ongoing agronomic effect of this on crop growth, as well as the flow on effects in terms of off-site impact. The spatial dependence of soil compaction will be directly investigated from the existing literature. It will then conduct a literature assessment of load, versus change in density, versus soil texture and published procedures on this topic. The review concludes by detailing the knowledge gaps, as well as the key soil properties and functions to test with respect to the hypothesis.

2.2 EFFECTS OF MACHINE STRESS ON SOIL MECHANICS

2.2.1 Stress in Soil

Soil compaction by wheeling of agricultural machines is the reduction of soil porosity as a product of axial and shear stresses propagating through the soil profile. The result of this is most critical in localized zones beneath the wheel soil interface and is often characterised by a visible rut on the soil surface (Défossez & Richard, 2002). Developing an appreciation for the stress strain relationships which account for this phenomenon creates an understanding of the foundation of soil compaction in agriculture. Early work by (Boussinesq, 1885) describes a solution to model the distribution of vertical stress as implied by an external load over the contact area. This model considers the medium to be a *"homogenous, isotropic, ideal elastic material"* (Boussinesq, 1885) which assumes complete uniformity throughout the entire soil profile (Soane & Van Ouwerkerk, 1994). The stress propagation which controls the volume is calculated using the following (Boussinesq, 1885) equation *(Equation 2.1)* and visually represented by *Figure 2.1*.

$$\sigma_1 = \frac{3P}{2\pi r^2} cos^3\theta \qquad \textit{Equation 2.1}$$

where,

σ_1= vertical stress, at distance r, under a point P, and θ is the angle between the radius and vertical.

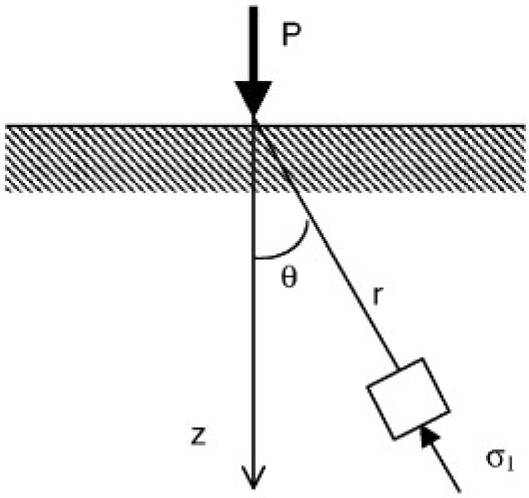

Figure 2.1 Stresses in a volume under a point of applied load (Défossez & Richard, 2002)

It was discovered that this model could be applied to soil (of varying soil strength) with the addition of a concentration factor, ξ as seen in *Equation 2.2* (Fröhlich, 1934), where soil characteristics (firmness) as a result of bulk density and moisture content are recommended as values 4, 5 and 6 for hard, firm and soft soils, respectively (Défossez & Richard, 2002).

$$\sigma_1 = \frac{\xi P}{2\pi r^2} cos^{\xi-2}\theta \qquad \textit{Equation 2.2}$$

where,

σ_1= principal stress, at distance r, under a point P, and θ is the angle between the radius and vertical.

This equation accurately relates an increase in concentration factor to deeper penetration of vertical stress within the profile. However, is limited to determining stress propagation by applied load from a single point as it radiates into the soil medium. (Söhne, 1953) recognised the inapplicability of this model as stress implied by agricultural tyres is presented by an area, rather than a single point. Hence, a modification of the Boussineq formula allows stress at the tyre- soil interface to be modelled by assuming an elliptical contact area. The distribution of vertical stress as a result of this is displayed in *Figure 2.2*.

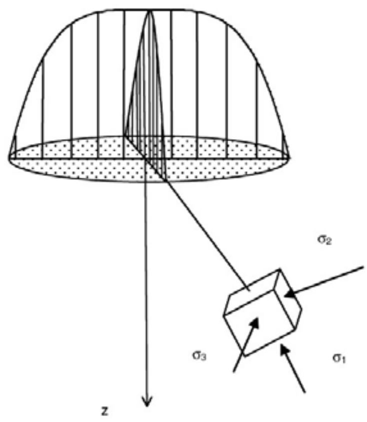

Figure 2.2 *Stresses acting on a volume of soil considering pressure distribution by a contact area between tyre and soil according to (Söhne, 1953), (Défossez & Richard, 2002).*

It is evident that shear stress due to wheeling involves horizontal momentum, enforcing triaxial loading. Ignored in the work by (Söhne, 1953), this was further extended by (Johnson & Burt, 1990) to improve the scope of this study. By once again considering stress to be a single shear point load, and following the Cerruti equation procedure, all three principal stresses, $\sigma_{1,}$ $\sigma_{2,}$ & σ_3 can be predicted for any point in the soil (Défossez & Richard, 2002). The accuracy of this was further improved by (O'sullivan et al., 1999) who assumed only $\sigma_{1,}$ to be vertical and $\sigma_{2,}$ & σ_3 to be longitudinal and transverse, respectively. More specifically, longitudinal and traverse stresses are derived from contact area, the shape of stress distribution and the magnitude of wheel slip (Défossez & Richard, 2002). Fitting a regression equation to these outputs develops *Equation 2.3* (O'sullivan et al., 1999).

$$\ln\left(\frac{\sigma_1}{\sigma_n}\right) = c_1 z - c_2 A + c_3 \xi \qquad \textit{Equation 2.3}$$

where,

σ_1= principal stress, σ_n = $\sigma_{2,}$ or σ_3, A = contact area, z = depth, ξ= concentration factor and c_1, c_2 & c_3 are regression constants.

This literature resonates the fundamental effects of machinery traffic on the soil medium. Furthermore, work presented conveys the importance of considering stress applied by wheeled traffic will not only remain within a localised zone and will propagate into the medium surrounds. A review of theory here reveals that soil compaction may be considered as uniaxial compression, however, stresses on the triaxial plane should be acknowledged for best applicability.

2.2.2 Hydraulic Properties

Soil infiltration can be defined as the process by which water on the soil surface penetrates the profile (Lili, 2008). This movement of water can be quantified as the soil's infiltration capacity, described as the "*maximum rate at which a soil when in a given condition can absorb rain as it falls"* (Horton, 1933). Conditions required to reach a soil's infiltration capacity include an excess of water on the soil surface to ensure constant surface moisture availability. Furthermore, it is evident that the infiltration capacity reduces exponentially with time and sample moisture content under these conditions as it approaches the soil's saturated hydraulic conductivity, (Ksat). Soil compaction by machinery traffic adversely affects soil hydraulic properties (Keller et al., 2019). This particularly inhibits plant available water (PAW) and the movement of solutes through the soil profile (Ankeny et al., 1990) as unsaturated water infiltration is reduced. It is suggested that this function is a product of soil pore alteration with machine induced stress. Work by (Ankeny et al., 1990) depicts tension infiltrometer testing across a range of tilled fields, subjected to varying degrees of wheeled traffic. It was concluded that large macropores within a soil profile are responsible for transporting the greatest proportion of hydraulic flow, but are most susceptible to degradation by machinery traffic. This is reinforced by (Keller et al., 2019) in an assessment of historical saturated hydraulic conductivity reduction with time as the mass of agricultural machinery has developed with the increased demand for production efficiency. The report describes that an arable soil today has a subsoil Ksat value approximately 40% lower than its natural benchmark condition, (represented by the year 1900 in *Figure 2.3*) based on calculations using the pedo- transfer function of (Wösten et al., 1999), incorporating bulk density.

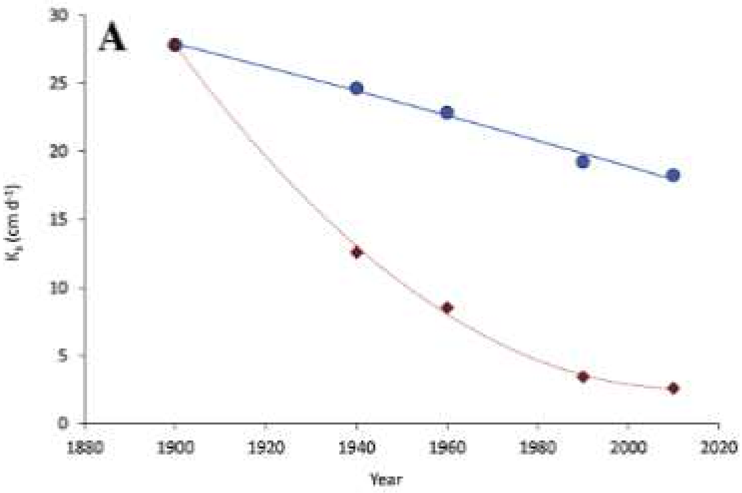

Figure 2.3 *Plot of reduction in Ksat in an arable subsoil caused by an increase in machinery weight (BLUE) based on relative bulk density (RED) as estimated by the pedo-transfer function (Keller et al., 2019).*

Although the data presented here is based on estimations it is clear that machinery-imposed stress reduces soil hydraulic potential. This is reinforced in experimental work completed by (Lebert & Horn, 1991; Wander et al., 2002) detailing the significance of these consequences when considering the effects of machine traffic on soil mechanics.

2.3 Agronomic Effects and Extent of Compaction

Soil compaction has an adverse effect on the agronomic system, limiting production by inhibiting plant growth. This is a direct result of the restricted plant root growth, (access to moisture and nutrient uptake) and available water within the soil profile, caused by a decrease in porosity, hydraulic reduction and structural degradation (Steffan & Schaefer, 2016). Cotton farming in Australia is particularly traffic intensive as growers often incorporate winter crops in rotation, and as a result, compaction is a primary concern. Degradation of soil physical properties as a result of compaction has been well documented (Antille et al., 2016; Bennett et al., 2017; Bennett, 2017; Braunack & Johnston, 2014) and are discussed earlier in this report. (Jamali et al., 2021) conveys the importance of also considering the effect of compaction on soil water dynamics. Crop water use, soil water recharge and resulting plant water stress relationships are critical factors for assessing overall productivity loss from soil compaction. Insufficient quantities of PAW cause stomatal closure, inhibiting photosynthesis and increasing crop water stress (Idso et al., 1977; Jackson et al., 1981). Additionally, this elevates canopy temperature as crops attempt to conserve water by limiting transpiration, reducing the rate of crop growth. A study by (Reichle et al., 2015) reported a heavy correlation between cotton yield and the cumulative time of optimal canopy temperature.

There is an abundance of research estimating the extent of soil compaction. Literature details compaction stresses nearing an extent of 200kPa is inferred at subsoil depths by large commercially available John Deere combines, (gross weight greater than 30T), (Chamen et al., 2015). Furthermore, similar results are reported for cotton pickers (equivalent mass) with onboard module building (Antille et al., 2016). Soil compaction induced by agricultural machinery can be described by the elastic and plastic deformation in relation to soil mechanics, (Défossez & Richard, 2002; Nawaz et al., 2013). The effects of compaction are largely reversible when compression is restricted to not exceed the soils elastic phase. However, failure occurs as the compression stress exceeds precompression stress and said soil reaches the plastic deformation phase (Bennett et al., 2014). This value, for Australian vertosols is said to be an average of 99.3kPa (Kirby, 1991). Thus, as the effects of compaction implied by most machinery, (excess of 10 Mg) is technically irreversible, alleviation techniques are regularly required. Natural amelioration of Vertosol compaction is a very gradual process, often taking upwards of 5 years under no-till conditions (Radford et al., 2007). This process is best accelerated by a number of farming practices including tillage, deep ripping or sewing a ley pasture. However, it is important to ensure adequate conditions, (soil moisture content) are prevalent when exercising these management options to ensure structural repair is achieved.

The effect of soil compaction from external loading decreases linearly with depth to an extent of 700mm for a given soil of medium texture, (Ansorge & Godwin, 2007; Antille et al., 2013). Considering a depth of 800mm to allows for a conservative prediction that applies to soils of varying consistency.

Generally, soil compaction from offroad vehicle traffic occurs as a triaxial force, exerted by a wheel travelling across the horizontal plane, under the influence of gravity. Towed wheels predominantly exert a vertical normal force to the soil whereas drive wheels exert additional shear forces (Alakukku, 1999). These shear forces can account for up to 50% of compaction effects within the topsoil region of a profile, (Raghavan et al., 1977). Triaxial tests available are accurate and produce results applicable to a variety of different soil conditions, however they are expensive. Uniaxial soil testing requires less input, is inexpensive, applicable to most modelling applications and further, sufficient for use in this study considering the varying soil types being examined will be collected individually.

The soil compaction occurring in agriculture is often in conjunction with lateral compression and non-volumetric changes to the soil structure as a result of a change in bulk density (Koolen & Kuipers, 1983). A range of factors influence the extent and characteristics of soil compaction including the soil type, soil condition, soil moisture content, magnitude of the applied force, and the quantity, duration of loading events (Alakukku, 1999). Research on soil moisture content suggests it is the most influential soil property when considering soil compaction extent as a result of affected soil strength (Dawidowski & Lerink, 1990). As the velocity of a machine is increased, the duration of the loading period is reduced proportionally, hence inferring less stress on the subsoil of a profile, (Alakukku, 1999). This effect is enhanced in soils that lack density.

Industry literature has investigated the implication and repercussion of vertical soil stresses. This has led to the development of comprehensive compaction models such as the SoilFlex model (Keller et al., 2007). A particular assessment made on the implication of machinery traffic on Australian soils suggest that vertical stresses of up to 200kPa are commonly experienced at depths of around 300mm in heavy Vertosols (rear axle), (Antille et al., 2016). The machine analysed in this study was the John Deere 7760 round bale cotton picker. Tyre parameters for this machine as recommended by the manufacturer are as follows: 520/85R42 R1 (inflation pressure: 0.25 MPa) and 520/85R34 R1 (inflation pressure: 0.32 MPa) for the dual drive and steering tyres, respectively (Deere and Company, 2014). Furthermore, these simulations derived that the minimum surface stress implied by this machine is at the tyre-soil interface is approximately 350 kPa. This contact stress occurs for each of the front drive tyres, (average wheel load: 5.43 Mg) which is considerably less than the rear steer tyres (average wheel load: 8.25 Mg) (Bennett et al., 2016). It is important to accurately consider these load values in the context of developing industry applicable study.

2.4 Off-Site Impact and Mitigation Techniques

2.4.1 Australian Cotton

The Australian cotton industry is one of the largest globally, earning around $2 billion in exports annually, (*CSIRO*, 2022). Australian cotton farmers have remained competitive by striving for higher yields and lower production costs. This has been achieved by an industry focus on plant breeding, improvements in both post- harvest and in-crop practices and an increase in the recognition of the significance of soil health. Despite this, a recent Australian industry survey reported 66% of assessed cotton farms were impacted by soil compaction (CCA, 2020) and globally, an estimated 68 million hectares of agricultural soils are affected by soil compaction from vehicular traffic (Nawaz et al., 2013). The loss of productivity caused by soil compaction is generally experienced over an extended period of time (Jamali et al., 2021). Hence, the significance of the issue is often overlooked. Local compaction also presents a tremendous cost to society, as profit reduction for growers is passed onto produce price (Graves et al., 2015). However, a lack of information of the extent and severity of compaction at a national scale means there is very little quantitative reports on this. Although outdated, a study by (Walsh, 2002) estimates the extent of the economic impact of compaction in Australian agriculture to be $850 million each year. It can be suspected that this number has significantly increased over the past two decades with the inflation of agricultural machinery mass as a result of the demand for greater production efficiency (Bennett et al., 2019). This warrants the application of a large proportion of resources towards mediating the effects of compaction.

2.4.2 Managing Compaction

Pursuit of enhancing operational efficiency has led to the development of higher capacity machines with the aim of reducing the required number of passes in a field. Profit margins have been greater in the modern age with the addition of on-board module building in cotton pickers (Bennett et al., 2015). This addition to the cotton-picking system eliminates the requirement of multiple machines in practice, (boll buggies, modules builders). However, the trade-off for a reduction of passes across the field is a significant increase in axle loading, (rear axle loading, 16.5 Mg of a total 36 Mg machine mass). Quantitatively, some studies (Chamen et al., 2015; Keller et al., 2007; Koolen et al., 1992) have reported increases in subsoil stresses (400mm deep) of over 1000% since the period of horse drawn implements. The consequences of this practice have prompted the adoption of a variety mitigation techniques including technologies to increase the area of wheel- soil interface and hence alleviate wheel contact pressure. In cotton operations this is evident by the addition of dual tyres fitted to the front axle of modern cotton pickers, and in some instances, tracked tractors for round bale and module handling.

In addition to wheel-soil interaction modifications, machinery used in cotton picking is often required to undergo modification with farm wide confinement of load-bearing wheels to permanent traffic lanes, or controlled traffic farming (CTF). CTF is an effective means of compaction management (Tullberg et al., 2007), designed to alleviate the effects of machinery traffic in regards to soil health and land degradation. The potential operation profitability of implementing a CTF system is assessed in (Kingwell & Fuchsbichler, 2011). The most obvious technical and scientific benefit of CTF is increasing crop yield via the benefits of eliminating soil compaction, (improving plant available water and nutrients, enhancing root and plant growth and reducing erosion and water logging).

Furthermore, semi-permanent tramlines within a paddock have proven advantageous by providing a more tractive surface, (reduced rolling resistance and wheel-slip) and reducing driver fatigue, (consistent guidance tracks). These are particularly beneficial during time restricted periods throughout the farming season. CTF is the primary recommendation for managing soil compaction in cotton-based systems as reported in the guidelines by SOILpak for Cotton Growers (Daniells et al., 1996). However, the Australian cotton industry has witnessed a relatively slow adoption of CTF, despite the abundance of advertised whole-farm benefits. This is likely due to the unsuitability of imported equipment from Europe and the USA, and hence the associated cost of conversion and machinery modification, (Chamen et al., 2015; Tullberg et al., 2007). Furthermore, such modifications to new equipment are likely to void machine warranties and compromise re-sale value, further deterring the transition.

Specific financial margins accompanied with the adoption of CTF in Australian grain cropping systems are analysed by (Kingwell & Fuchsbichler, 2011). The study utilises a whole-farm bioeconomic model labelled known as the 'Model of an Integrated Dryland Agricultural System', (MIDAS) to provide a comprehensive comparison of the implementation of CTF. The investigation selected three theoretical dryland farming operations to address light sandy soil types and heavier clay rich soils by running season simulations for each, with and without the adoption of CTF. The results of the simulation suggested the majority of the profit increase can be attributed to enhanced grain revenue (yield and grain quality) which equates to roughly $31/ha compared to the $15/ha decrease in input costs from adopting the CTF system. It is also apparent that an increase in crop dominance within the farm plan will proportionally increase profits when adopting CTF. Whole farm effects of CTF include more regular cropping in areas with heavy clay soils to ensure a greater degree of profit, opposed to the lighter sandy soils where the benefits of CTF are less visible. This is particularly relevant when assessing the value of this system for implication on heavy clay soil mediums in cotton growing regions of Australia.

2.5 Spatial Dependence of Soil Compaction

2.5.1 Sub-field Constraint Variability

Spatially variable fields can also be defined by local areas of agricultural land which exhibit geographical deviation in both chemical and physical properties throughout the entire depth of the soil profile. If characterised soil properties limit crop growth and hence hinder agricultural production, they are classed as a constraint (Dang, 2022). Soils in dominant cotton growing regions of Australia are particularly susceptible to structural degradation. Hence, soil constraints such as salinity, acidity, subsoil compaction and sodicity are particularly prone to inhibiting soil infiltration and water storage attributes (Page et al., 2018). These effects compromise crop growth and hence yield, the primary consideration of farm management, which is rarely considered in a spatial context (Tilse et al., 2022). This literature suggests research should be targeted to develop a greater understanding of the interactions and associated consequences of these constraints.

Sub-field scale-based soil maps compiled from both predicted and measured datasets of soil physical and chemical properties are a highly valuable planning and educational tool. However, local variability of soil characteristics described by (Dang, 2022) mean it is often challenging to class a constraint type across a field in a particular category (Bennett, 2022). This is further complicated when considering soil property variability with depth within a profile. Soil profiles with significantly different properties between topsoil (0-20cm depth) and subsoil (>20cm depth) often naturally occur in Australia. Therefore, it is important to acknowledge the effects of constraining properties at each soil layer in the root zone. Vertosols found in Australia are generally alkaline and hence display dispersive properties due to associated sodium and potassium carbonates. Dispersiveness of a soil is ranked from values 0-16 by (Hazelton & Murphy, 2016) and include descriptions such as 'non-dispersive', 'mechanically dispersive' and 'spontaneously dispersive' derived from observations of the soil aggregates when immersed in solution. In addition to this, soils which display structural deterioration and evidence of waterlogging can be refined in class based on the soil pH (Bennett, 2022). As such, neutral dispersive soils occupy a pH between 6 and 8, thus imposing minimal anionic effects to crops grown in this soil. As pH exceeds these values, the soil is described as alkaline dispersive (Hazelton & Murphy, 2016) at this condition, excessive carbonates have toxic effects on plants. High clay content soils which are non- dispersive (do not slake or disperse in water) may be classed as saline with an electrical conductivity rating (1:5, dS/m) greater than 0.7 (Hazelton & Murphy, 2016; Shaw et al., 1994). Plant growth is constrained in these soils with regards to the osmotic effects of excessive salts. Despite these refined descriptions of constraining conditions within a soil profile, there is an absence of literature investigating perpetual relationships between these characteristics and a soils susceptibility to compaction.

2.5.2 Spatial Variance of Soil Compaction

Studies surrounding the spatial effects of soil compaction can also be conducted by measuring changes in physical soil properties and identifying the associated behavioural patterns in soil profiles affected by compaction. A variety of sources have proven the adverse effects of heavy machinery in an agricultural system, particular in regards to soil productivity (Soane & Van Ouwerkerk, 1994). This is largely due to the decrease in a soils microporosity when it is in a compacted state, and the restricted nature of gaseous and hydraulic exchanges that follow. A study by (Barik et al., 2014) directly addresses the relationship between field traffic operations and the degradation of soil physical properties, particularly those which indicate compaction issues (aggregate stability, bulk density, total porosity, penetration resistance and moisture content). Furthermore, it concludes that among these properties, aggregate stability and penetration resistance are affected the most dramatically from repeated field traffic. Kriging is an effective method of displaying the results of these affected soil profiles, (Barik et al., 2014) as it enables the model to be analysed on all three planes to determine the exact locations of spatial variance throughout the profile.

It is evident that this project will need to take into consideration the abundance and type of plant cover in the trial sites. Penetration resistance is generally decreased in soils with plant cover, (Pinzón-Gómez et al., 2016) this is likely to affect the spatial moisture content of the system and potentially dictate the varying levels of compaction. Furthermore, studies have shown that in these circumstances, compaction levels often increase with depth whilst the moisture content acts inversely proportional. These soil profile properties will be measured and potentially accounted for throughout the different sites addressed in the study.

2.5.3 Spatial Mapping of Soil Compaction

As technology develops and allows for an increased uptake of soil data, the industry has looked for viable options to support large quantities of information, and further present information on a broad platform. Soil science has thus propelled the development of primary digital mapping technologies such as geographic information systems (GIS), remote locating systems (GPS) and a variety of data sources such as those composed by digital elevation models. A review on the development of spatial soil prediction reveals the relative inaccuracy of available soil maps to be accounted for by the extensive labour and cost of completion on site soil surveys. Hence the demand for spatial soil prediction, specifically via GIS platforms presents a number of mathematical models suggesting quantitative relationships are most evident between soil topography but should not be assumed to be linear and soil can be predicted spatially from geographic position using a variety of pedometric techniques. As such, these approaches are generally based on *Equation 2.4* where a soil at location (x, y) is dependent on the geographic coordinates (x, y) and the characteristics of the soil at an adjacent location $(x + u, y + v)$ (McBratney et al., 2003).

$$S = f(x, y), s(x + u, y + v) \qquad \textit{Equation 2.4}$$

A review on digital soil mapping (McBratney et al., 2003) recalls the development of spatial prediction models from the Jenny (1941) equation for mechanistic soil modelling. The primary of these being the SCORPAN model, a spatial prediction function which considers the following soil/ environment relationships, as detailed in the review (McBratney et al., 2003), *"soil, other or previously measured attributes of the soil at a point; climate, climatic properties of the environment at a point; organisms, including land cover and natural vegetation; topography, including terrain attributes and classes; parent material, including lithology; age, the time factor; space, spatial or geographic position".* Mathematically, the function is described by the *Equation 2.5*.

$$Sa = f(s, c, o, r, p, a, n) + e \qquad \textit{Equation 2.5}$$

Where, any soil property, 'Sa', at a certain point is a product of the soil properties at that location based on: space (s), climate (c), organisms (o), relief (r), parent material (p), age (a), and auto-correlated errors (e). Successfully executing the steps of this model offer the potential to produce both digital and dynamic soil maps. These maps display soil constraints, attributes and types and are stored and utilised on GIS platforms to promote effective data analysis and assessment. Further, the model offers an approach to extrapolating existing soil maps in the currently unmapped areas. An application of this is depicted in (Bui et al., 1999) where 's' for a previously mapped soil is carried through to an unmapped area, so no new sampling is required.

Application of this theory in developing delineating maps of soil compaction has little applicability due to the dynamic nature of the constraint (Alaoui & Diserens, 2018). Furthermore, considering the long set nature of soil compaction, particularly in the subsoil, detailed knowledge of previous land uses should be taken into account, a resource which is often scarce. The extent of this long memory effect is highlighted by (Zimmermann et al., 2006) in a study reporting the impact of 13 years of cattle grazing on soil hydraulic properties was still evident after a further 10 years of forest growth within a field. This infers a comprehensive soil map should include both short and long-term changes to soil condition. This is further complicated by apparent variability of soil compaction in both time and space (Alaoui & Diserens, 2018). Correlations between persistently compacted areas and limited yields have been acknowledged in studies by developing 3D models of a soil profile by measuring cone resistance (an empirical and cheap method of quantitating soil compaction) and indicator kriging, (a geostatistical technique of developing a visual model). A study by (Castrignano et al., 2002) identified the presence of these infield relationships within a derum wheat crop. Similarly, the practicality of sampling cone resistance for the evaluation of soil compaction at depth is concluded. The results from this study highlight the desirability of a minimal degree of soil compaction, as this promotes sufficient structural stability in plant establishment. It also depicts the effectiveness of geostatistical techniques in measuring soil compaction across both vertical and horizontal profiles. Whilst this article notions the importance of considering several contributing factors (nutrient deficiencies, seeding rates, etc.) when acknowledging spatially varying yields, the impacts of applied mechanical stress is not addressed. Extending this work would require the sampling of a similar dataset but with concern to the outcomes of machinery traffic. More specifically, there is no widely accepted method to measure the mechanical properties of a soil that directly reflect the risk for compaction with field traffic (Alaoui & Diserens, 2018).

2.6 Relations Between Load, Change in Density and Soil Texture

Geometric distribution of machine mass is responsible for the magnitude of wheel axle loads endured by the soil medium in an agricultural field. This loading has a direct relation to change in soil bulk density (Horn et al., 2003). This is proven by experimental procedure, (Horn & Fleige, 2003) where measurements of soil bulk density were repeatedly recorded with continuing passes of agricultural machinery, (tractor with rear axle load of 11 Mg). The results highlight that at all depths within a soil profile, soil bulk density increases with the number of passes. Additionally, after 10 passes, the same bulk density was recorded for all depths of the given soil profile.

A relationship can be drawn between a soil's vulnerability to compaction and its specific texture composition (Nawaz et al., 2013). However, this susceptibility is largely affected by the moisture content of the soil at the instance of compaction. (Horn et al., 1995) explains that at low moisture contents, silt loam soils with low colloid contents are exposed to a greater risk of compaction in comparison to medium or fine textured clay loam soils, whilst sandy soils are generally less susceptible to compaction. An experimental study to determine the contributing factors to the degree of soil compactness, (Arvidsson, 1998) found that bulk density of soil in its reference state increased with increasing sand content. This can be accounted for by the lack of micropores in sandy soils, (Koolen & Kuipers, 1983). The study measured bulk density at different field sites before and after machine traffic. The results however, did not reveal any significant correlations between the degree of compactness after traffic and the differing mineral fractions of the soil (Koolen & Kuipers, 1983). The lack of variance here was contributed to consistency in field moisture content. In general, all soils are less susceptible to compaction at very low moisture contents rather than high (Gysi et al., 1999). However, a reduction in compressibility is experienced as the moisture content exceeds the point where all soil pores are filled with water (Smith et al., 1997). This is reinforced in work by (Ishaq et al., 2001) where bulk density is used to quantify compaction extent as moisture content increases in a given soil, as detailed in *Figure 2.4*. The results of this study conclude that for the sandy clay loam repeatedly compressed with consistent load, bulk density increases with moisture content up to a limit, after which it decreases.

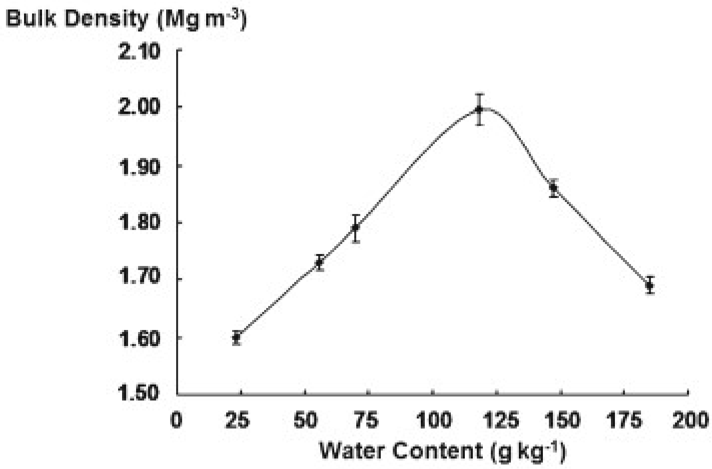

Figure 2.4 *Relationship between soil water content and bulk density for analysis of compaction (Ishaq et al., 2001).*

In addition to soil water content and texture, soil organic matter has been shown to affect the degree of compactness after exposure to vehicular traffic load (Nawaz et al., 2013). However, laboratory simulation of varying soil organic matter content in soil is a restricted exercise and published work is limited.

2.7 Uniaxial Compression Testing

The concept of uniaxial compression is a procedure that can provide a quantitative measure of the degradation of a soil via implied load. The varying influence of machinery traffic on soil health and crop yield is examined in procedure by (Håkansson, 1990). In particular, the continuous loosening of the soil structure by tillage and decrease in soil volume with seasonal agricultural practice. The soil moisture relationship throughout the cropping season also has a significant effect on the optimal degree of compaction, (Edling & Fergedal, 1972; Håkansson et al., 1988). The water in moist soil acts as a lubricant between soil particles (Suzuki et al., 2013). This in turn enhances deformation and results in an increase in soil bulk density. It is evident, because of this, the influence of machinery traffic can have varied effects of the degree of soil compactness and hence accurate simulation of these scenarios require extensive experimentation. Measuring results for these procedures is most appropriately achieved by recording volumetric relationships, such as bulk density or total porosity (Håkansson et al., 1988). It is important to consider soil physical properties when analysing results of this nature, particularly texture as relative bulk density values may vary between soil types, hence indicating different degrees of compactness. Uniaxial compression as described by (Håkansson et al., 1988) involves applying pressure by a plate within a cylindrical sleeve to a volumetric soil sample collected from the plough layer (approximately 27cm depth) within a field. The plate is covered with a 7mm rubber mat and the soil is thoroughly moistening and allowed to equilibrate. This study focuses on comparing the dry bulk density of the compressed samples for a range of moisture contents. It is considered that this procedure is less laborious (than traditional proctor compaction tests) and hence the preferred method for effectively characterising the degree of compactness of soil samples in this format. Furthermore, application of external load allows for the implication of a range of stress states at the soil surface. This allows for a comprehensive dataset of simulated machine traffic of differing mass. However, (Arvidsson, 1998) compares this uniaxial compression procedure to reference field bulk densities (Håkansson et al., 1988) after actual machine wheeling, revealing variance in results. The study concludes that from the significance of measured differences, the uniaxial compression tests was an insufficient means of predicting the effects of compaction in the field.

2.8 Hydraulic Conductivity

The infiltration rate or flux is the measurement of water traversing through the soil surface at any given time. Typically recorded in a dimension of length per unit time, devices known as infiltrometers have been developed to measure this phenomenon. Infiltrometer types include the single ring, double ring, tension or disk and hood infiltrometers. Possibly the most common procedure for estimating soil hydraulic properties consists of two concentric metal rings that are inserted into the soil surface. Recording the reduction of water level after filling both the outer and inner rings can be used to determine the sample Ksat. Disk infiltrometers consist of a cylindrical reservoir filled with water, supported by a permeable disk base. The rate of water infiltration is determined by the decrease in water level, hence producing cumulative curves to further depict soil hydraulic properties (Latorre et al., 2013). Despite these efforts, variability in results is not uncommon amongst differing infiltration methods, especially in regards to values for saturated hydraulic conductivity (Lai & Ren, 2007). This can be accounted for by the application of mechanical loads in the process of ring insertion and the variance in contact material used in tension infiltrometers (Lili et al., 2008).

Mini-disk infiltrometers (MDI's) are able to record a large quantity of measurements over a short period of time, hence producing a comprehensive dataset. The measurement is made using transient data as infiltration approaches stabilisation. It is also apparent that the automation of MDI's is an effective technique to improve experimental accuracy and productivity. This can be achieved via a pressure transducer and accompanied datalogger to record electrical pulses with pressure change. Measurements of infiltration into unsaturated soil can be used to calculate soil hydraulic conductivity, a function of water potential and soil water content (Zhang, 1997). To achieve this, *Equation 2.6* is fitted with recorded measurements of cumulative infiltration against time.

$$I = C_1 t^{1/2} + C_2 t \quad \text{Equation 2.6}$$

Where, C_1 is associated with hydraulic conductivity and C_2 is the soil sorptivity. The hydraulic conductivity (K) is the derived from a separate equation as follows.

$$K = \frac{C_1}{A} \quad \text{Equation 2.7}$$

Where, C_1 is the slope of the gradient of the cumulative infiltration curve against the square root of time and A is a value which relates the van Genuchten parameters for a given soil to the suction and radius of the infiltrometer disk (*METER*, 2022). Hydraulic conductivity at both saturated and unsaturated conditions provides a valuable parameter for consideration by land owners, managers and scientists. More specifically, nutrient transport and fluctuations in soil moisture by both ground water recharge and precipitation can be predicted by infiltration characteristics.

2.9 Soil Stress State Modelling

The calculated surface stress of a soil is dependent on what stress state model is used. Thus, to accurately take a quantitative assessment of the degradation of a soil profile, a specific soil stress state model must be assumed across all calculations in the investigation. Furthermore, it is apparent that the variance across these models will result in comparative discrepancies. Since the development of foundations made by (Rankine, 1857; Roscoe, 1968), there has been a considerable quantity of resources directed towards the modification and testing of the theory of plasticity in geomechanics (Gens & Potts, 1988). The derivative of initial critical state (CS) state models were the series of cam-clay formulations (Roscoe, 1968) which consisted of basic mathematical descriptions of the yield surface, hardening and plasticity and elastic volumetric strains (Gens & Potts, 1988) of a soil structure. The refinement of this model to achieve greater similarity between computed and observed soil stress states has led to a variety of theoretical models however, the simplicity and accuracy of one of the earliest CS models; modified cam-clay (Roscoe, 1968) has been predominately adopted in studies of varying contexts for decades. The model's success is attributed to the elliptical yield locus developed to overcome drawbacks presented within the yield surface by the original model (Gens & Potts, 1988) however, the suitability of different models across soil types is noted.

Whilst sufficient in most applications, the modified cam-clay model can be further refined by the application of a new stress tensor developed from the Mohr Coulomb criterion, (Yao & Sun, 2000). Opposed to the cam-clay model, (which considers the material to behave as a frictional fluid of constant volume) this modification implies an additional failure criterion to the ultimate failure of a soil. Derived from the more closely approximated Mohr- Coulomb criterion, with a constant angle of internal friction, the transformed stress tensor is introduced to enable greater accuracy in the description of triaxle compression, and also extension of clay soils. By adopting the transformed stress tensor, the model is able to satisfy the consistency from shear yielding to shear failure of soils in the revised model.

Establishing an accurate representation of the stress- strain relationships in soil behaviour is critical when developing a model to represent field compaction. Elementary methods of both practically and theoretically measuring stress and strains within soil have been reviewed by authors (Horn et al., 2003). It is explained in this study that devices used tended to cause significant disturbance in the soil sample structure, altering the natural benchmark condition of the test. The application of these results in a ubiquitous fashion is therefore unreliable. Studies derived by, (Lipiec & Hatano, 2003) have then proceeded to develop thorough comparisons between these techniques and more modern technologies like pressure transducers and optical fibre position laser sensors. This assessment revealed that the correct application of these sensory techniques allows for the precise detection of stress and displacement variations at different soil depths under both laboratory and field conditions, providing results that replicate the stress applied by moving wheels. These results concluded that both soil stress and displacement are largely influenced by the loading, water content and soil type. The relevance of these studies is identified in the methodology of quantifying these soil properties. The intent of this project is to analyse these values when influenced by excessive external mechanical stresses and determine the relative importance of these properties when considering soil compaction mitigation techniques.

2.10 Thesis Rationale

There have been numerous reports looking into the various factors limiting crop growth on a sub-field level. It has been established that soil compaction is the most severe of these constraints, particularly in the Australian cotton industry. The importance of developing a thorough understanding of the relations between machine traffic, soil property and compaction extent is well documented in current literature. Furthermore, a proportion of these studies have addressed the rates of spatial compaction, compared these results to the structural properties of the soil profile and even to the productivity of the field.

It is apparent however that the research on quantifying soil compaction extent as affected by spatial variability at the sub-field scale with respect to soil type and soil constraint changes has failed to be accurately compared to the mechanical stress imparted by machine traffic in any one trial. Furthermore, industry literature on the mapping of physical soil properties is limited. This is a product of lacking an understanding of the interactions between in situ spatial mapping of soil compaction and other soil constraints. This knowledge gap has led to an industry perception that sub-field soil constraint variability is the predominant attribute restricting crop yields.

Uniaxial compression testing for soil compaction is much less laborious and more reproducible than a standard proctor test, (Håkansson, 1990). It allows for efficient simulation of compaction instance whist controlling key soil properties and test parameters. To develop an accurate assessment of the variability in soil compaction impact with respect to spatial and constraint variation several functions should be considered. These include but are not limited to, sample moisture content, applied stress state for compaction simulation and the resultant hydraulic properties of the sample. Appropriate testing of these key soil properties is crucial in determining the magnitude of mechanical stress imparted by machine traffic and additionally, whether or not this outweighs the effect of spatial variability of soil constraints within a soil type at the sub-field level.

3. METHODOLOGY

3.1 AIMS AND OBJECTIVES

This study aims to test the alternate hypothesis, that there will not be any significant variability in soil compaction impact for a given moisture content spatially within a given soil type, with respect to the degradation implied by machine traffic. In order to achieve this, the soil compaction extent as affected by spatial variability at the sub-field scale with respect to soil type and soil constraint changes for a variety of sites must be quantified.

From a total of four sites, to consider changes in geolocation, this project will spatially diagnose the soil type and constraint variability. In addition to this, samples will be tested for compaction experimentation under laboratory conditions, for a range of moisture contents and stress states. This will allow for a thorough analysis of the variation in the samples' infiltration properties, and the associations and effects on the pore geometry in the soil profile for the varying stress states. Ultimately providing an outcome to be considered by land holders for future management practices.

3.2 PROCEDURE

The key tasks for this project can be categorised into 4 phases as described below;

- Phase 1. Site selection and diagnostics
- Phase 2. Monitoring point identification and sample collection
- Phase 3. Uniaxial compression testing
- Phase 4. Infiltration testing

3.2.1 Site selection and sub-field diagnostics

Spatially varying soil types across Eastern Australia offer contrasting properties in a physical, chemical and biological sense. To maintain the applicability of this study to the broader focus of Australian agriculture, the site selection aimed to include an array of soil types. More specifically, these soil types were selected based on the regular mediums experienced by Australian cotton growers. Consequently, the total 16 sites analysed in the Cotton Research and Development Corporation funded project USQ1903, led by Prof. John McLean Bennett, were assessed. The location of these sites was spread across North West NSW and Southern Queensland regions. The project provided the necessary data for a complete spatial diagnosis of the soil type and soil constraint variability at the sub-field scale was completed for each field. The project data was derived from a total of 20 samples spatially distributed at each field. The samples were collected by a soil core sleeve, (ID of 43mm) on a utility-mounted hydraulic coring apparatus and stored in sampling bags. From each of these samples, separate sections were analysed from depths 0–10 cm, 10–20 cm, 40-50 cm and 60-70 cm. A comprehensive dataset for each field was developed from the measured soil pH, exchangeable sodium percentage (ESP), aggregate stability and cation exchange capacity (CEC) for each sample. This provided the necessary context to derive a subfield analysis for each location. A numerical constraint value, (0-16) was then assigned for each of the 20 sample points, for all 16 fields based on the characteristics of pH, salinity, sodicity, and stability of both the top and subsoil at each location. For example, a soil with a constrain value of 14 was described as having a top soil which is alkaline and non-dispersive and a subsoil which is Alkaline dispersive (mechanically dispersive, salinity with depth).

Of the 16 assessed sites, only four offered more than three sub-field constraint classes. Three of these sites were thus selected based on fulfilling criteria with the fourth chosen due to geographic convenience. The first two sites selected, field 3 and field 4 are located approximately 12 km South-West of Dalby, QLD, managed by growers Shawn Fresser and Steve McVeigh respectively. Fields 7 and 8 are located approximately 6 km South-East of Talwood QLD, managed by growers Ben Turner and Tom Seerey, as seen in *Figure 3.1*. The climates of these locations consist traditionally of long hot summers and cold clear winters. The majority of seasonal rain falls during the summer months with Talwood (Goondiwindi airport) averaging a slightly higher yearly rainfall than Dalby (Dalby airport), 593.9mm and 619.4mm respectively, (*Australia's official weather forecasts & weather radar - Bureau of Meteorology*, 2022). All fields endure seasonal cotton crops and are irrigated via a flood/ furrow system.

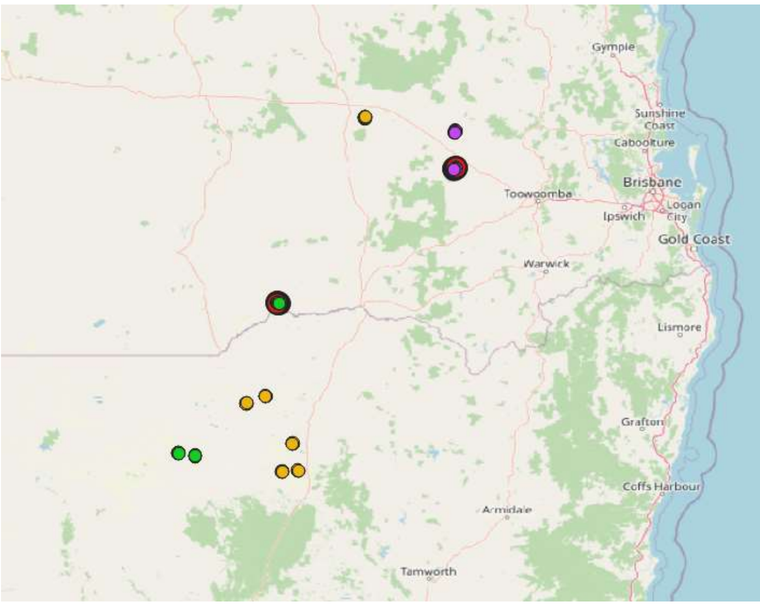

Figure 3.1 *Geographic location of all 16 experimental sites analysed in the USQ1903 CRDC project with the RED outline detailing the sites selected from this project and changes in sampling point colour indicating varying constraint values of each point.*

3.2.2 Monitoring point identification and sample collection

Four monitoring points at each field were selected to provide results that compare the significance of soil characteristic change and compaction outcome. Furthermore, the monitoring points were chosen to depict both spatial and soil constraint class difference and hence represent sub-field variability as displayed in *Figure 3.2*.

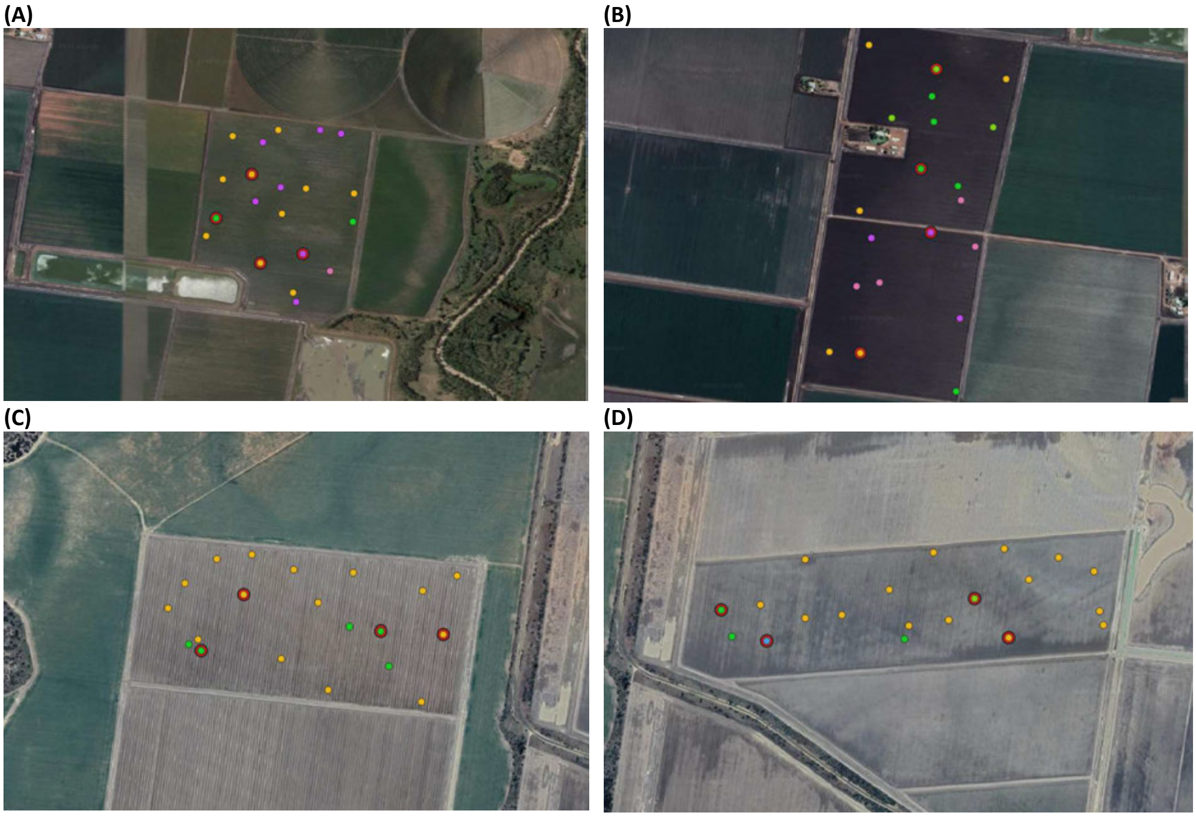

Figure 3.2 *Experimental sites (A) DALBY- Shawn Fresser Field 3, (B) DALBY- Steve McVeigh Field 4, (C) TALWOOD- Ben Turner Field 7, and (D) TALWOOD- Tom Seerey Field 8, detailing the 20 sampling locations from the USQ1903 CRDC project, with red outline indicating the locations selected for this project. Changes in sampling point colour indicate the describing constraint value as seen in the legend below.*

LEGEND

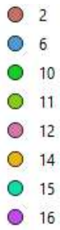

Where, 2 = acidic dispersive topsoil/ alkaline dispersive subsoil, 6 = neutral dispersive topsoil/ alkaline dispersive subsoil, 10 = alkaline dispersive topsoil/ alkaline dispersive subsoil, 11 = alkaline dispersive topsoil/ neutral dispersive subsoil, 12 = alkaline dispersive topsoil/ non-dispersive subsoil, 14 = non-dispersive topsoil/ alkaline dispersive subsoil, 15 = non-dispersive topsoil/ neutral dispersive subsoil, 16 = non-dispersive topsoil/ non dispersive subsoil.

Using a Trimble GPS unit and portable receiver to locate each of these points (*Figure 3.3- (A)*), a field-based analysis of the clay content and natural density with depth was conducted to improve the reliably of the soil profile characteristics obtained via coring and determine the most suitable soil profile locations for sampling. Soils with significant clay content variation with depth require a quantity of top and sub-soil to assess for each point. Soils which are relatively uniform (vertosols) only require representative soil from the top soil. For each of the 16 monitoring points, an approximate field state volume of 15000 cm^3 (0.274 x 0.274 m soil pit, *Figure 3.3- (B)*) was extracted from the topsoil, (0-20 cm depth) to maintain consistency with the known data set. This volume was selected to ensure an excess of data was available for after the soil was cleaned of trash in addition to the nine samples (approx. 750 cm^3 each) used for uniaxial compression. The soil was extracted by a shovel and stored in labelled hessian bags. Fields 4,7 and 8 had been recently formed into raised beds for planting in a flood/ furrow irrigated system. Field 3 was occupied by standing cotton stubble (flood irrigated) which had been harvested in months prior. The absence of tillage in this field accounts for the higher field moisture content at the time of sampling. Mixing of the topsoil throughout storage was not a concern as tillage to these depths is a frequent practice and the effects of compaction are relatively consistent with sample depth in a uniform soil (Bennett et al., 2019).

(A) **(B)**

__Figure 3.3__ (A) Handheld Trimble GPS unit and receiver alongside sample collection apparatus, (B) soil pit from which sample was collected (volume approx. 15000 cm^3). Both images are taken at location: TALWOOD- Ben Turner Field 7.

3.2.3 Uniaxial compression testing

3.2.3.1 Deriving Target Moisture Contents

Before uniaxial compression testing, the range of moisture contents were assumed. Three moisture contents for each monitoring point were selected to produce a proper representation of the compression curve. After collection from the field, samples for each monitoring site were oven dried at 40 degrees celcius (*Figure 3.4- (A)*) as described in (Blake & Hartge, 1986) to later meet targeted moisture contents using a known volume of water. This method is preferred to drying samples to 105 degrees celcius as extreme temperature has the potential to create additional covalent bonds within clay soils, hence baking can produce errors in compression results. Moisture content fluctuations from atmospheric humidity were mediated by ensuring samples were not left openly exposed for an extended period of time and containers were sealed where possible. These discrepancies were regarded as experimental error and ignored in the results. Two sub- samples were extracted for the determination of each soil's moisture content at 40-degree celcius, and the Atterberg limits for each monitoring site. Ambient air (40-degree celcius) moisture content was calculated for each soil by drying a small subsample to 105 degrees celcius in container of known volume and inputting the recorded masses into the *Equation 3.1*.

$$Mc = \frac{Ws - Ds}{Ws} \quad \textit{Equation 3.1}$$

Where, Mc = moisture content, Ws = mass of wet soil and Ds = mass of dry soil.

Atterberg limits were determined for each soil following standard procedures, (AS 1289.3.1.1-2009 and AS 1289 3.1.1, 3.1.2). For the plastic limit, approximately 40 g of moistened soil is kneaded between the fingers and palm. About 8 g of material is rolled into a thread. If the thread crumbles at 3mm diameter, the plastic limit has been reached (*Figure 3.4- (C)*) and the broken threads are collected, weighed and dried to determine the moisture content. If the material crumbles before it reaches 3 mm diameter, it is too dry, if the thread rolls down to 3 mm without crumbling the material is too moist. The plastic limits were recorded for a sample of each of the 16 monitoring points for later simulation in compression testing.

The liquid limit test involves moistening the sample until the material becomes a thick homogeneous paste. The sample was then placed in the cup of a calibrated Casagrande device and flattened parallel to the base using firm downward pressure to ensure the exclusion of air voids. The material is divided using the grooving tool (*Figure 3.4- (B)*) and handle turned at a rate of 120 revolutions per minute until the two halves of the sample come into contact for a length of 10mm. At this time, the number of blows is recorded and a sample is extracted from the centre of the cup for the determination of the moisture content. The test is repeated 4 times at slightly higher moisture contents. The intent of the test is to have four evenly spaced moisture contents over a range of between 40 and 15 blows. The moisture contents and corresponding number of blows are plotted as seen in the example below (*Figure 3.4- (D)*) and a line of best fit is produced to deduce the moisture content that equates to 25 blows. This is the liquid limit of the soil.

(A)

(B)

(C)

(D)

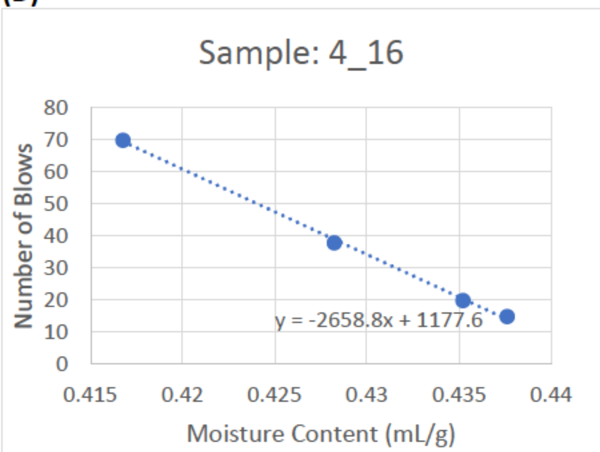

Figure 3.4 *Procedure for sample analysis (A) labelled samples in soil oven, drying to 40 degrees celcius, (B) Casagrande apparatus used to determine sample liquid limit, (C) crumbling samples rolled to 3mm diameter, indicating sample plastic limit, (D) plot of moisture content versus the number of blows observed in the Casagrande procedure used to determine sample liquid limit.*

After the plastic and liquid limits were recorded for the samples at each site, the three gravimetric moisture contents were assumed. For each individual soil, this was the plastic limit, the average of the plastic and liquid limit, and the difference between those values, as seen in *Table 3.1*.

Table 3.1 *The three target gravimetric moisture contents, assumed for each sample before uniaxial compression testing.*

Sample ID	*MC 1 (MC3-MC2)*	*MC 2 (Plastic Limit)*	*MC 3 (Average of Atterberg Limits)*
3_12	9.14%	20.18%	29.32%
3_18	10.56%	16.51%	27.07%
3_3	8.58%	18.06%	26.64%
3_9	9.34%	23.82%	33.16%
4_15	10.96%	22.42%	33.38%
4_16	10.74%	21.85%	32.59%
4_6	10.66%	20.09%	30.75%
4_9	11.39%	20.28%	31.66%
7_18	9.21%	17.79%	26.99%
7_20	9.39%	17.97%	27.37%
7_6	9.78%	16.63%	26.40%
7_7	9.02%	18.76%	27.78%
8_1	9.17%	18.23%	27.39%
8_3	8.44%	19.62%	28.07%
8_7	8.73%	18.08%	26.81%
8_9	9.03%	19.96%	29.00%

3.2.3.2 Sample Preparation

Each sample was ground (*Figure 3.5- (A)*) with sufficient energy to traverse through a 6.7mm sieve (*Figure 3.5- (B)*) in order to remove stones, in line with (Håkansson, 1990), the energy applied was monitored to ensure excessive force did not compromise the physical bonds of the smaller aggregates. After grinding, a gravimetric mass of 600g from each sample was weighed and placed in beaker. The required mass of water required to achieve each target moisture content was calculated from the ambient air moisture content. The soil and water were gradually combined in a 150mm long PVC cylinder (86.2mm inside diameter), (*Figure 3.5- (C)*), sealed using a plastic wrap sheet and elastic band and left to equilibrate for 24 hours (*Figure 3.5- (D)*). Each cylinder was dropped 10 times from a height of 50mm to attain uniform packing. Care was taken to ensure the soil was moistened uniformly throughout using a spray bottle applicator. This was repeated for three replicates of each moisture content, for each sample (144 total).

__Figure 3.5__ Sample preparation procedure (A) soil grinder set to an opening of 10mm to break down large aggregates/ clods, (B) 6.7mm sieve used to filter trash and stones from field samples, (C) apparatus used for uniaxial compression sample preparation in PVC cylinder, (D) samples moistened, sealed and left to equilibrate for 24 hours before uniaxial compression.

3.2.3.3 Compression Testing

Uniaxial compression tests were repeated for a variety of moisture contents and stress states to simulate a comparison between the effects of machinery traffic of different mass, passing over the field at varying degrees of saturation. The press used for uniaxial compression testing was a 50 kN MATEST CBR Tester screw type press (*Figure 3.6- (A)*), fitted with a load cell and linear variable differential transformer (LVDT) to record both load and deflection data. A 10mm steel disk (86mm diameter) was used as the interface to simulate soil compaction. The loading for each compression test was designed procedurally to simulate a single pass of heavy machinery and provide comparison to Suzuki et al. (2013). Bonded to the steel disk used to compress the soil within the sleeve was a layer of 6mm rubber *Figure 3.6- (B)*), to create a sufficient seal with the PVC pipe, ensure that the moist soil would not stick to the piston after compression and to mimic the soil/ tyre interface which would occur in a field. During testing, each sleeve was inserted within a steel proctor mould and 90mm bore casing to support the walls of the PVC sleeve under loading (*Figure 3.6- (C)*). The tests were designed to measure the overall compression (deflection) of the soil within the sleeve as each loading force was applied. This was recorded digitally using catmanEasy V4.1.1 software (*Figure 3.6- (D)*). Each stress was not maintained for an extended period of time as such the soil was allowed to rebound, as it would in a field scenario, after a compaction incident from machinery traffic. A sample for each of the three moisture contents from each monitoring site was loaded to each of the following pressures, 50kPa, 100kPa, 350kPa. These values represent a load less than the literature recommended stress, the recommended stress threshold and the minimum implied stress from machine loading, (John Deere 7760), respectively. From these pressures, the corresponding loads implied by the press in uniaxial compression can be calculated from the 86.2mm diameter of the sample, as seen in *Table 3.2*.

***Table 3.2** Pressures required to simulate target stress states and corresponding loads.*

Pressure (kPa)	***Force (kN)***
50	0.292
100	0.584
350	2.04

After compression, each sample was resealed to maintain the target moisture content. The change in density was then calculated for each sample from the extent of deflection.

(A)

(B)

(C)

(D)

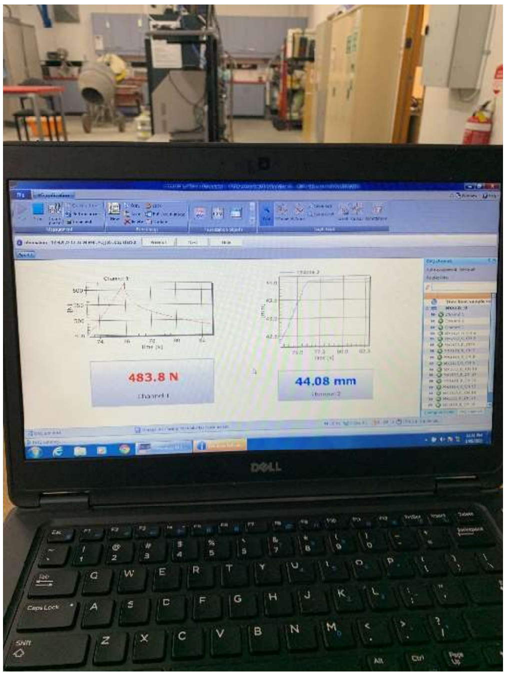

Figure 3.6 *Uniaxial compression procedure (A) 50 kN MATEST CBR Tester screw type press, (B) 6mm rubber disk bonded to 10mm steel spherical plate used to compress soil, (C) steel proctor mould and 90mm bore casing used to support sample in compression, (D) catmanEasy V4.1.1 program used to record test outputs, load and deflection.*

3.2.4 Unsaturated Hydraulic Conductivity

3.2.4.1 Infiltration

A series of 9 Automated Mini-disk Infiltrometers (AMDIs) were used to measure the transient water infiltration for each of the compressed samples (stored at target moisture contents). The ADMIs were each equipped with a differential pressure transducer (model: *Honeywell ABPDRRV001PDSA3*) to convert pressure into and electrical signal, connected to a datalogging microprocessor (model: *Adafruit Feather M0 Adalogger*) to record the signal. The body of the infiltrometers were an acrylic plastic and assembled to match *Figure 3.7*.

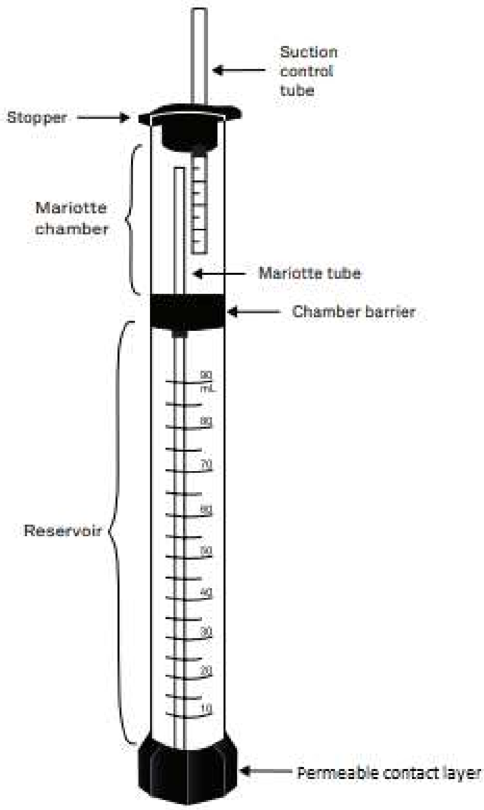

Figure 3.7 *Diagram of mini disk infiltrometer used to measure infiltration rates in soil.*

With the Mariotte Chamber filled to control suction, the suction tube was inserted to attain a suction rate of 2cm (*METER*, 2022). The main reservoir was filled with rain water (distilled water may change ionic balance in clay soils, causing dispersion) before a nylon fabric was fixed with elastic to the bottom of the chamber, creating a permeable contact layer. A thin layer of fine silica sand was placed on the surface of each compressed sample to ensure sufficient hydraulic contact (*Figure 3.8- (A)*). Ensuring the infiltrometer made a solid contact with the soil surface, one of the 9 ADMIs were positioned on each of the compressed samples, inducing infiltration into the soil as the water leaves the lower chamber (*Figure 3.8- (B)*). The pressure measured in the water column has a linear relationship with water height, when graphed against time, this can be used to calculate hydraulic conductivity. Measurements from the differential pressure transducer were recorded every 5 seconds from the beginning of each infiltration procedure and saved to an SD card for later processing.

(A) **(B)**

Figure 3.8 *Apparatus used to measure soil infiltration rates (A) samples prepped for infiltration testing with a thin layer of silica sand, (B) nine AMDIs in place and recording infiltration rates on compressed samples.*

3.2.4.2 Data Processing/ Calculations

The data for cumulative infiltration with time was uploaded and processed using (*RStudio Team*, 2015). As the soil types in this study were particularly susceptible to structural deterioration as soil moisture increases, infiltration results often indicated there had been a break in hydraulic contact (infiltrometer and soil interface). This meant that an analysis of each raw dataset was required and cleaning of inaccurate sections of the infiltration curves was completed where appropriate, as described in *Figure 3.9 (A)*, a break in hydraulic contact occurs at approximately 3100s, thus data points after this timestamp should be removed. Also, comprehensive data cleaning would see the initial three data points removed to improve the accuracy of the gradient of the cumulative infiltration curve against the square root of time which is later computed from this dataset. Disparity is often evident in initial data points in this procedure as the surface sand is quickly saturated at the beginning of the infiltration test. The measured data in *Figure 3.9 (B)* effectively illustrates the water infiltration with time, no significant inconsistencies are present and hence filtering is not required.

(A)

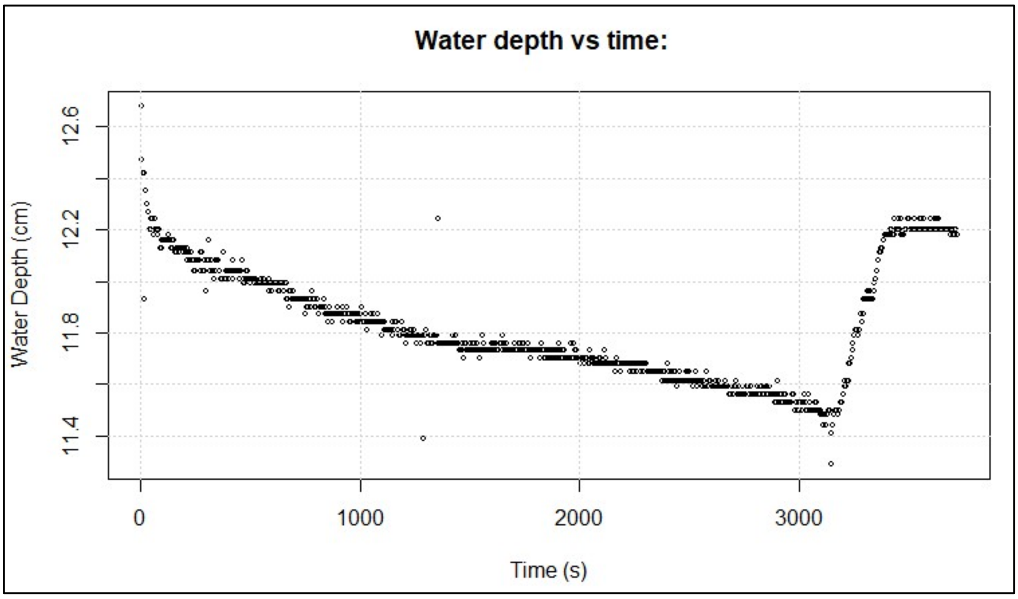

(B)

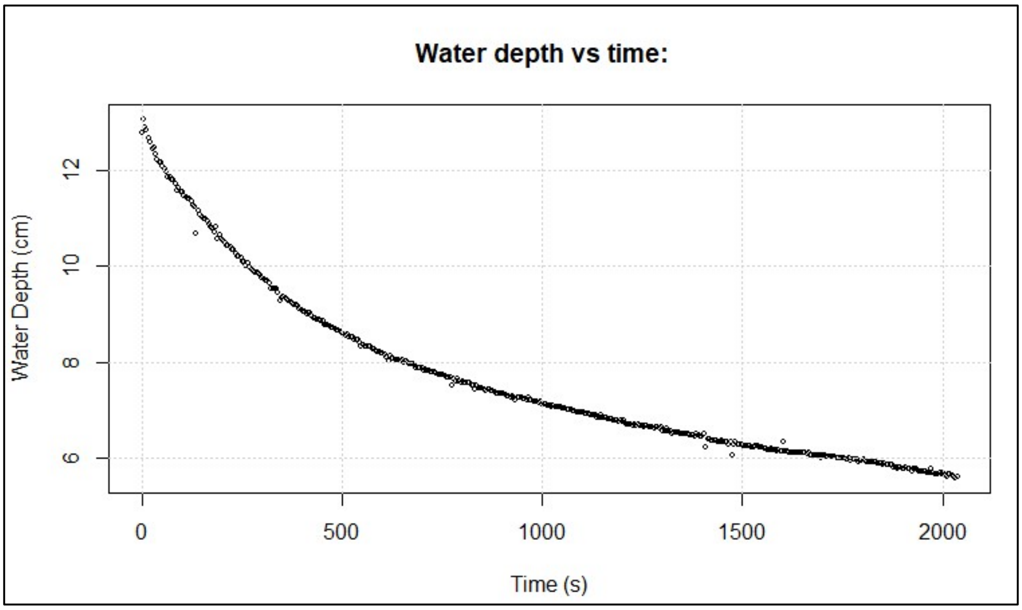

Figure 3.9 *Plots of cumulative infiltration with time (A) example of a test requiring data cleaning (break in hydraulic contact occurs at t = 3100s), (B) example of a test which does not require data cleaning.*

Unsaturated hydraulic conductivity, Ku was calculated by first examining filtered cumulative infiltration versus time using the two-term infiltration equation (*Equation 3.2*). This equation is commonly used (Kargas et al., 2017; Madsen & Chandler, 2007) calculate hydraulic conductivity from mini disk infiltrometers.

$$I = C_1 t^{1/2} + C_2 t \qquad \textit{Equation 3.2}$$

Where, C1 is associated with hydraulic conductivity and C2 is the soil sorptivity. After disregarding deficient or inaccurate datasets and cumulative infiltration curves which produced negative gradients, only 117 (81.3%) sufficient values remained for soil hydraulic conductivity calculation. The hydraulic conductivity (K) is the derived from a separate equation, (*Equation 3.3)*.

$$K = \frac{C_1}{A} \qquad \textit{Equation 3.3}$$

Where, C1 is the gradient of the cumulative infiltration curve against the square root of time, computed using RStudio, and A is a value which relates the van Genuchten parameters derived from characterisation data for a given soil to the suction and radius of the infiltrometer disk (*METER*, 2022). The van Genuchten parameters for soil hydraulic properties were using Rosetta Handbook software (*Rosetta*, 2022) for calculated bulk densities and average field texture of each compressed sample. It is important to note that this software considers textural classes in line with the USDA/FAO soil particle size classification system, hence data collected in alternate formats must be converted for this application.

3.3 Health, Safety and Ethics Clearance

Several personal risks were entailed by the above procedure and hence were considered and evaluated in order to evade the occurrence of any serious incidents. Laboratory procedures involve proceeding with caution when operating in close proximity to the soil oven set to 105 degrees celcius. Soil trays were left to cool momentarily after drying in order to avoid burns. Similarly, the grinder used for preparing sample posed significant risk if operated incorrectly. To comprehend this, soil was manipulated using specified tools to avoid limbs coming into close proximity to the machine opening. Ethics clearance was exercised when gaining permission and access to fields from growers in the soil sampling process. Furthermore, access to the CAE's soil sampling utility (Can-Am) was authorised and arranged with assistance from USQ staff.

4. Results

The purpose of this section is to highlight key findings from the study and establish relevant trends within the datasets. The following analysis provides a means to quantify soil compaction extent as affected by spatial variability at the sub-field scale and further, an accurate representation of soil-water characteristics of the field.

4.1 Soil Properties

The relevant physical and chemical properties of the soils tested are presented in the tables below. The Atterberg limits (plastic and liquid limits) of all soils found in this study are generally lower than other published results from studies in similar geographical locations, (Bennett et al., 2019). It can be observed that Atterberg limits are moderately lower for the Grey Vertosols at the Talwood sites, (Site 7 and 8) than the Black Vertosols at the Dalby sites, (Site 3 and 4). It is important to note that Atterberg limits remain relatively consistent throughout each field despite soil constraint variability. All results for the soil physical properties exhibit a degree of consistency, reinforcing the validity of the procedure.

Vertosols in Queensland are often sodic and Alkaline, (Biggs et al., 2010) this is evident throughout all of the soils analysed in this study. Furthermore, these soils generally display dispersive properties due to associated sodium and potassium carbonates. The tables below describe these characteristics commonly occurring in both the top and sub-soil sections of the profile. In addition to this, a diagnosis of several sites revealed an increase in salinity with depth. These results are based upon electrical conductivity readings of the sample in solution and can inhibit the growth of sensitive crops. Salinity can be introduced to the soil profile by ground water sourced irrigation procedures.

Table 4.1 *Soil properties from monitoring points at site 3.*

Location: Dalby		***Site Number: 3***		***Soil Type: Black Vertosol***		***Average field texture (SSC): (45, 13, 43)***
Sample ID	**Longitude**	**Latitude**	**Plastic Limit (MC)**	**Liquid Limit (MC)**	**Constraint Class**	**Constraint Description: Top soil/ Sub soil**
3_3	151.181	-27.247	18.1%	35.2%	10	Alkaline dispersive / Alkaline dispersive (highly saline)
3_9	151.184	-27.249	23.8%	42.5%	16	Alkaline Non-dispersive / Alkaline Non-dispersive (strongly alkaline throughout, potential dispersion)
3_12	151.182	-27.249	20.2%	38.5%	14	Alkaline Non-dispersive / Alkaline dispersive (mechanically dispersive, salinity with depth)
3_18	151.182	-27.245	16.5%	37.6%	14	Alkaline Non-dispersive / Alkaline dispersive (mechanically dispersive, salinity with depth)

Table 4.2 Soil properties from monitoring points at site 4.

Location: Dalby		***Site Number: 4***		***Soil Type: Black Vertosol***		***Average field texture (SSC): (33, 13, 55)***
Sample ID	**Longitude**	**Latitude**	**Plastic Limit (MC)**	**Liquid Limit (MC)**	**Constraint Class**	**Constraint Description: Top soil/ Sub soil**
4_6	151.167	-27.257	20.1%	41.4%	16	Alkaline Non-dispersive / Alkaline Non-dispersive (high to excess salinity at depth, potentially dispersive)
4_9	151.164	-27.262	20.3%	43.1%	14	Alkaline Non-dispersive / Alkaline dispersive (strongly alkaline)
4_15	151.166	-27.255	22.4%	44.3%	10	Alkaline dispersive / Alkaline dispersive (highly saline)
4_16	151.167	-27.251	21.9%	43.3%	11	Alkaline dispersive / Neutral dispersive

Table 4.3 Soil properties from monitoring points at site 7.

Location: Talwood		***Site Number: 7***		***Soil Type: Grey Vertosol***		***Average field texture (SSC): (35, 13, 53)***
Sample ID	**Longitude**	**Latitude**	**Plastic Limit (MC)**	**Liquid Limit (MC)**	**Constraint Class**	**Constraint Description: Top soil/ Sub soil**
7_6	149.514	-28.510	16.6%	36.2%	10	Alkaline dispersive / Alkaline dispersive (highly saline)
7_7	149.517	-28.510	18.8%	36.8%	14	Alkaline Non-dispersive / Alkaline dispersive (mechanically dispersive, salinity with depth)
7_18	149.508	-28.509	17.8%	36.2%	14	Alkaline Non-dispersive / Alkaline dispersive (saline throughout)
7_20	149.507	-28.511	18.0%	36.8%	10	Alkaline dispersive / Alkaline dispersive (highly saline)

Table 4.4 Soil properties from monitoring points at site 8.

Location: Talwood		***Site Number: 8***		***Soil Type: Grey Vertosol***		***Average field texture (SSC): (25, 18, 58)***
Sample ID	**Longitude**	**Latitude**	**Plastic Limit (MC)**	**Liquid Limit (MC)**	**Constraint Class**	**Constraint Description: Top soil/ Sub soil**
8_1	149.535	-28.513	18.2%	36.6%	14	Alkaline Non-dispersive / Alkaline dispersive (mechanically dispersive, salinity with depth)
8_3	149.524	-28.512	19.6%	36.5%	10	Alkaline dispersive / Alkaline dispersive (highly saline)
8_7	149.534	-28.512	18.1%	35.5%	11	Alkaline dispersive / Neutral dispersive
8_9	149.525	-28.513	20.0%	38.0%	6	Neutral dispersive / Alkaline dispersive (salinity at depth)

4.2 Uniaxial Compression

This section presents plots of the bulk (dry) density of the compressed sample, and the three target moisture contents (assuming no moisture loss during equilibration) for each monitoring point (soil type). The bulk density is calculated from a measured mass of each sample at it's know ambient air moisture content. Each series describes a different stress state applied to the soil surface, (50, 100, 350 kPa) assumed by compressing each sample with the required load, 292, 584 & 2040 N respectively. These applied load values are calculated from the soil surface area within the 90mm PVC (86.2mm ID).

The majority of compaction curves are parabolic and open downwards. The apex of each of these indicates the optimal moisture content (OMC) of the soil. Critical state parameters of soils in this region were analysed by (Kirby, 1991). This study found the average OMC to be slightly less than average plastic limit of those soils. This is also evident in the plots below, and thus can be considered an appropriate relationship for heavy clay soils. Several datasets display a linear curve or a parabola which opens upwards. These results are irregular, possibly a product of inaccurate data and can be considered inconclusive. Unlike a standard proctor test to develop compaction curves, the measured data points in this uniaxial compression procedure does not provide a comprehensive display of data. To ameliorate this error, a greater number of samples at different moisture contents should be tested and assessed.

A common relationship that can be identified across all plots is the convergence of each stress state towards a common bulk density as moisture content increases. This highlights the dependence of moisture content on a soil's susceptibility to compaction. In addition to this, the bulk densities observed for samples exposed to a stress state of 350 kPa are significantly greater than replicates subjected to 100 kPa of stress. This is an appropriate relationship as this magnitude of pressure certainly exceeds the precompression stress of the soil. All trends observed from the plots are relatively similar for the extent of each field, with the exception of monitoring point 7_18 indicating high susceptibility to compaction. Furthermore, these tendencies are generally consistent across all fields, suggesting that the magnitude of stress has an overriding effect on soil compaction.

(A)

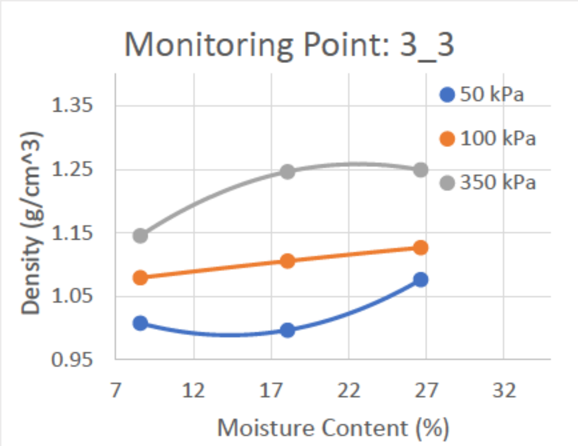
Monitoring Point: 3_3
Density (g/cm^3)
1.35
1.25
1.15
1.05
0.95
7
12
17
22
27
32
Moisture Content (%)
50 kPa
100 kPa
350 kPa

(B)

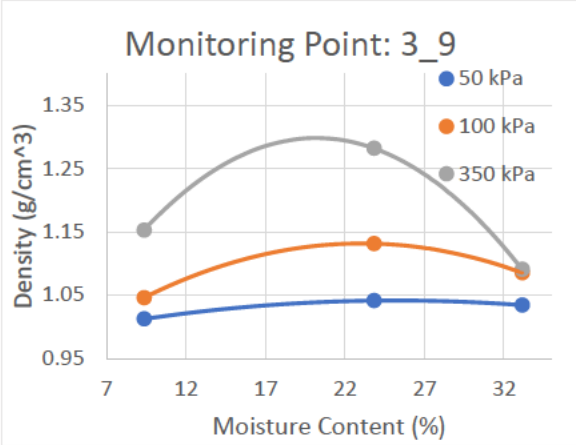
Monitoring Point: 3_9
Density (g/cm^3)
1.35
1.25
1.15
1.05
0.95
7
12
17
22
27
32
Moisture Content (%)
50 kPa
100 kPa
350 kPa

(C)

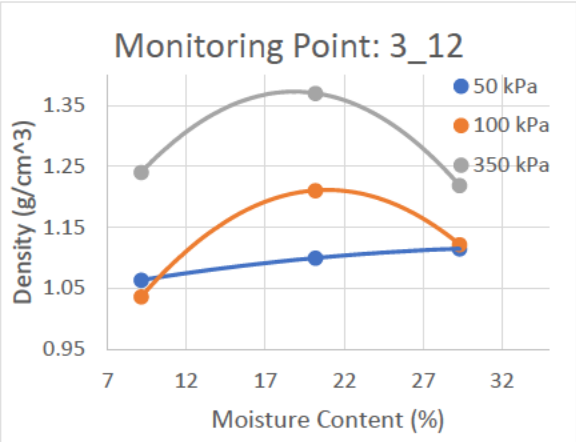
Monitoring Point: 3_12
Density (g/cm^3)
1.35
1.25
1.15
1.05
0.95
7
12
17
22
27
32
Moisture Content (%)
50 kPa
100 kPa
350 kPa

(D)

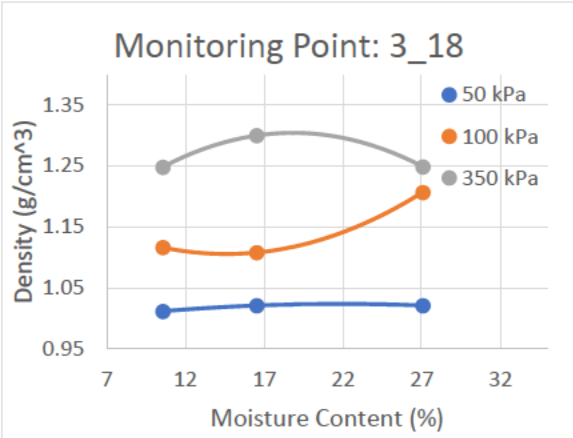
Monitoring Point: 3_18
Density (g/cm^3)
1.35
1.25
1.15
1.05
0.95
7
12
17
22
27
32
Moisture Content (%)
50 kPa
100 kPa
350 kPa

(E)

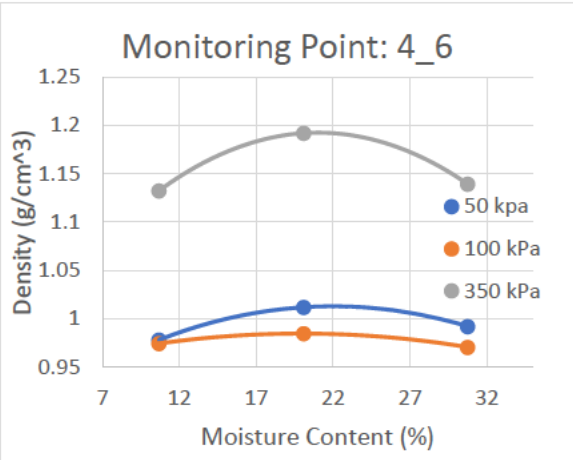
Monitoring Point: 4_6
Density (g/cm^3)
1.25
1.2
1.15
1.1
1.05
1
0.95
7
12
17
22
27
32
Moisture Content (%)
50 kpa
100 kPa
350 kPa

(F)

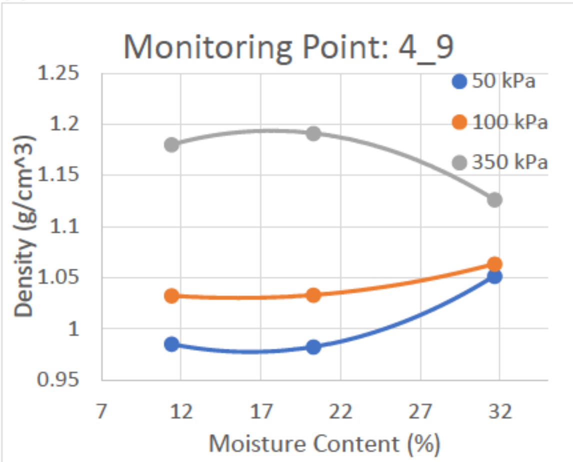
Monitoring Point: 4_9
Density (g/cm^3)
1.25
1.2
1.15
1.1
1.05
1
0.95
7
12
17
22
27
32
Moisture Content (%)
50 kPa
100 kPa
350 kPa

(G)

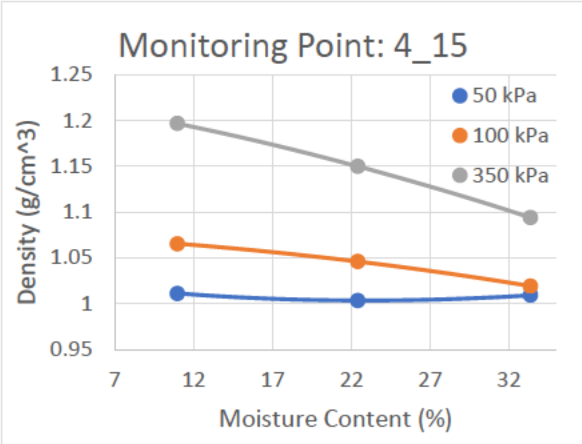
Monitoring Point: 4_15
Density (g/cm^3)
Moisture Content (%)
50 kPa
100 kPa
350 kPa
1.25
1.2
1.15
1.1
1.05
1
0.95
7
12
17
22
27
32

(H)

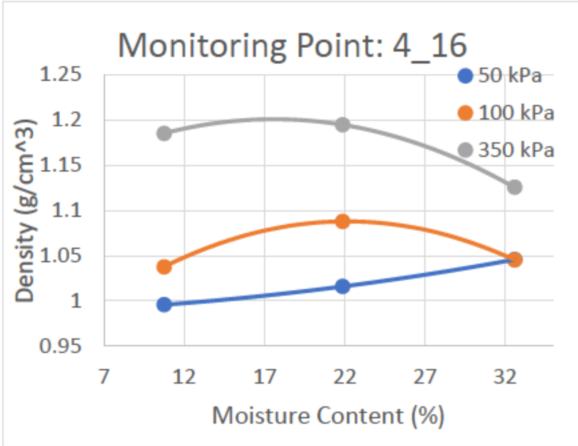
Monitoring Point: 4_16
Density (g/cm^3)
Moisture Content (%)
50 kPa
100 kPa
350 kPa
1.25
1.2
1.15
1.1
1.05
1
0.95
7
12
17
22
27
32

(I)

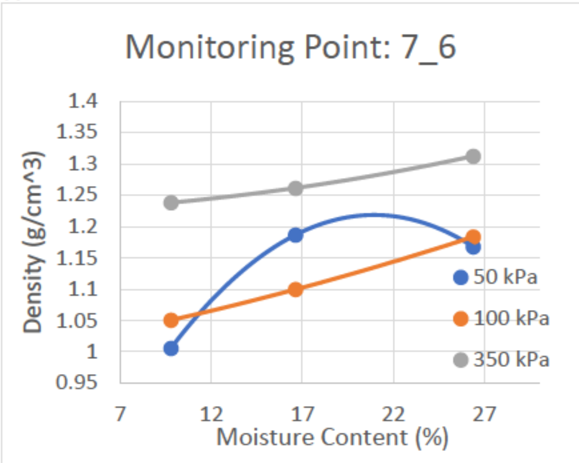
Monitoring Point: 7_6
Density (g/cm^3)
Moisture Content (%)
50 kPa
100 kPa
350 kPa
1.4
1.35
1.3
1.25
1.2
1.15
1.1
1.05
1
0.95
7
12
17
22
27

(J)

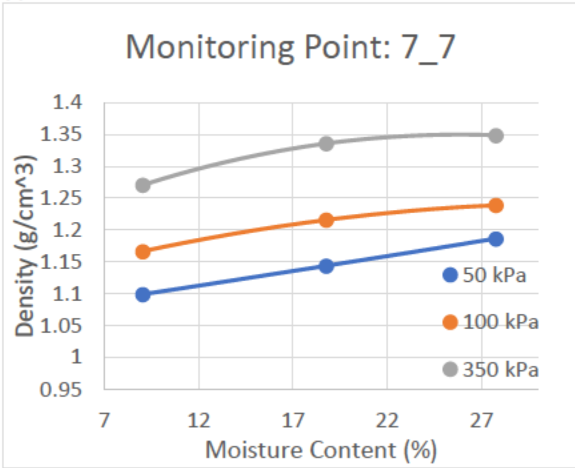
Monitoring Point: 7_7
Density (g/cm^3)
Moisture Content (%)
50 kPa
100 kPa
350 kPa
1.4
1.35
1.3
1.25
1.2
1.15
1.1
1.05
1
0.95
7
12
17
22
27

(K)

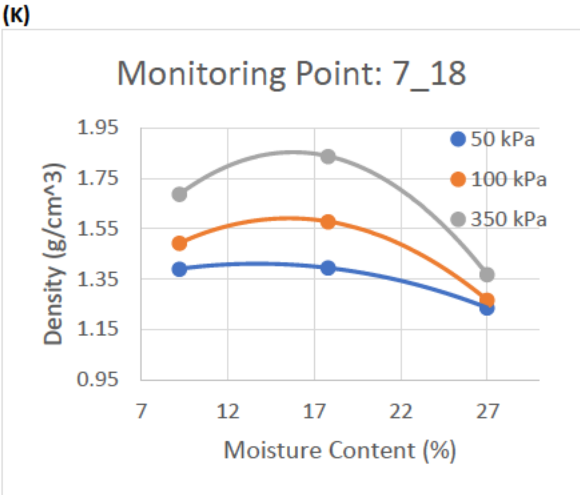
Monitoring Point: 7_18
Density (g/cm^3)
Moisture Content (%)
50 kPa
100 kPa
350 kPa
1.95
1.75
1.55
1.35
1.15
0.95
7
12
17
22
27

(L)

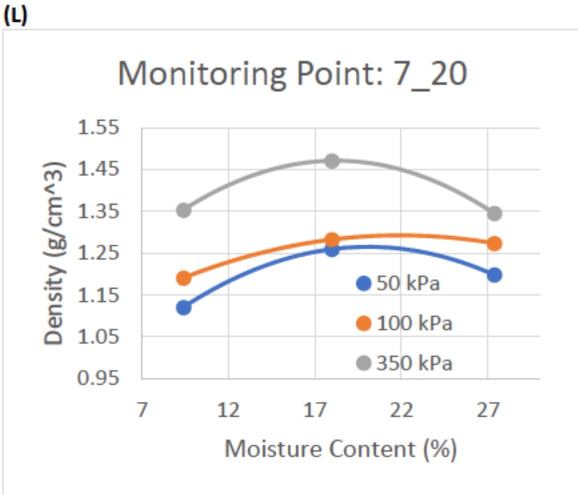
Monitoring Point: 7_20
Density (g/cm^3)
Moisture Content (%)
50 kPa
100 kPa
350 kPa
1.55
1.45
1.35
1.25
1.15
1.05
0.95
7
12
17
22
27

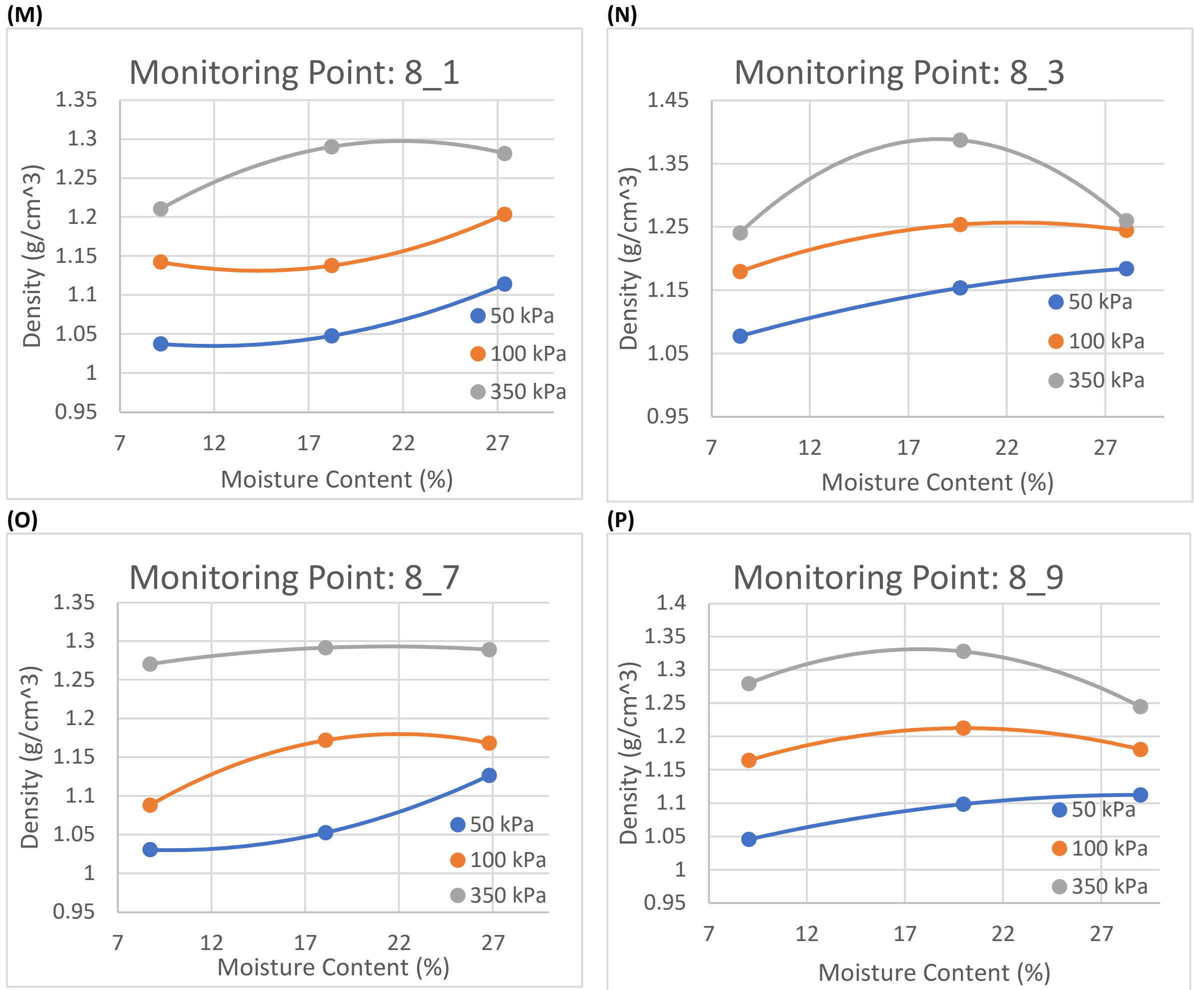

Figure 4.1 *Compression curves from uniaxial compression tests completed for the following: (A) SAMPLE 3_3, (B) SAMPLE 3_9, (C) SAMPLE 3_12, (D) SAMPLE 3_18, (E) SAMPLE 4_6, (F) SAMPLE 4_9, (G) SAMPLE 4_15, (H) SAMPLE 4_16, (I) SAMPLE 7_6, (J) SAMPLE 7_7, (J) SAMPLE 7_18, (K) SAMPLE 7_20, (L) SAMPLE 8_1, (M) SAMPLE 8_3, (N) SAMPLE 8_3, (O) SAMPLE 8_7, (P) SAMPLE 8_9 detailing the change in bulk density as moisture content increases for each of the 3 stress states.*

4.3 Soil Hydraulic Properties

This section presents the observed unsaturated hydraulic conductivity, K measurements for each soil type plotted against the moisture content, for each stress state. Hydraulic conductivity is calculated from measured cumulative infiltration versus time (recorded with mini-disk infiltrometers) using the two-term infiltration equation and related van Genuchten parameters.

Possibly the most predominant trend visible in the plots below is the tendency for all curves to converge towards a similar value of hydraulic conductivity as moisture content increases. This can be accounted for by the reduction in soil porosity associated with an increase in bulk density. Also, after the uniaxial compression procedure, samples were once again sealed to maintain target moisture contents, therefore, the existing water in the sample will deter infiltration, particularly in soil with dispersive tendencies. This relationship indicates that the moisture content of the subject soil has the greatest influence on compaction vulnerability and accordingly, soil hydraulic conductivity.

It is critical to acknowledge the absence of several datapoints in the plots below. As mentioned above, approximately 20% of recorded tests were deemed unsuitable for representation in this study. This primary cause of inaccuracy in results was the break in hydraulic contact during infiltration tests as the subject soils would swell with induced moisture. A more thorough analysis revealed that this often prevailed more than once in a particular soil type, indicating the structural instability of the medium. The soils from monitoring points, 7_20 and 8_3 are appropriate examples of this.

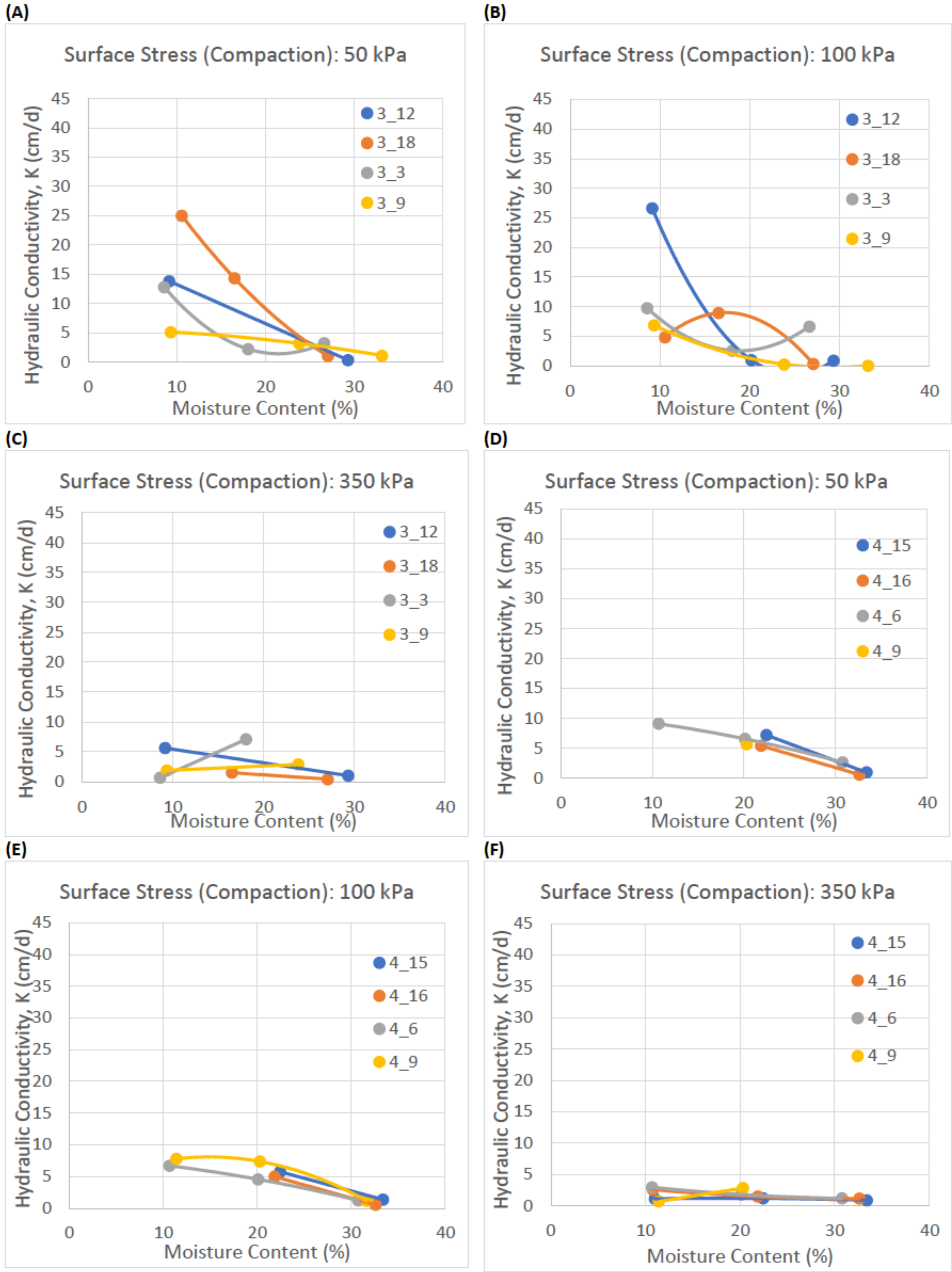

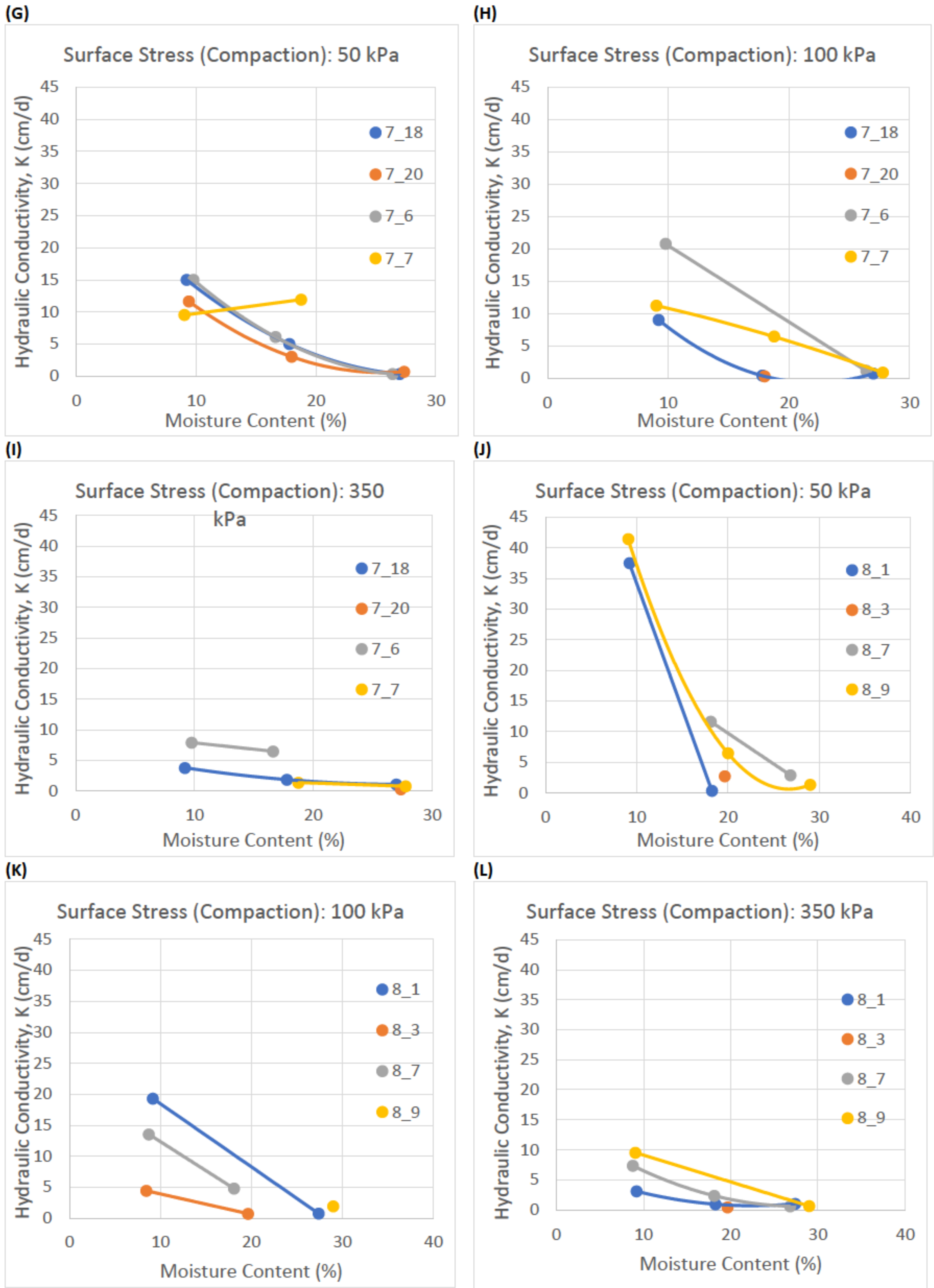

***Figure 4.2** Hydraulic conductivity plots (A) samples from field 3, stress state: 50 kPa, (B) samples from field 3, stress state: 100 kPa, (C) samples from field 3, stress state: 350 kPa, (D) samples from field 4, stress state: 50 kPa, (E) samples from field 4, stress state: 100 kPa, (F) samples from field 4, stress state: 350 kPa, (G) samples from field 7, stress state: 50 kPa, (H) samples from field 7, stress state: 100 kPa, (I) samples from field 7, stress state: 350 kPa, (J) samples from field 8, stress state: 50 kPa, (K) samples from field 8, stress state: 100 kPa, (L) samples from field 8, stress state: 350 kPa detailing the near saturated hydraulic conductivity of compressed samples at the 3 selected moisture contents.*

4.4 Spatial Variance

To convey a visual representation of spatial relationships of compaction extent on the subfield scale, field maps are included below. Each figure depicts the relative location of each monitoring point, in each field, as well the plastic limit and hydraulic conductivity of a soil sample collected from that point. The value for hydraulic conductivity is measured after simulated machine induced compaction (stress state of 350 kPa) at each soil's specific plastic limit.

Aside from a single monitoring point (7_6), these results exhibit a lack of spatial variance in relative hydraulic conductivity. In addition to this, the values for hydraulic conductivity are considerably less than idealistic and are likely to inhibit crop growth with low permeability.

(A)


3_18
PL=16.5% K=1.48
3_3
PL=18.1% K=0.63
3_9
PL=23.8% K=2.87
3_12
PL=20.2% K=2.46

(B)


4_16
PL=21.9% K=1.46
4_15
PL=22.4% K=1.18
4_6
PL=20.0% K=1.80
4_9
PL=20.3% K=2.8

(C)

(D)

Figure 4.3 *Experimental sites (A) DALBY- Steve McVeigh Field 3, (B) DALBY- Shawn Fresser Field 4, (C) TALWOOD- Ben Turner Field 7, and (D) TALWOOD- Tom Seerey Field 8 with the red points detailing the relative location of each selected monitoring point, in each field. The text conveys the results found for plastic limit and hydraulic conductivity of a soil sample collected from that point. The value for hydraulic conductivity is measured after simulated machine induced compaction (stress state of 350 kPa) at each soil's specific plastic limit.*

4.5 Statistical Analysis

4.5.1 Analysis of Variance

Single repetitions are used throughout all procedures in this investigation, which is standard for soil mechanics with this quantity of variables. In order to derive mathematical results applicable to the study hypothesis, and analysis of variance (ANOVA) was conducted for quantitative results relating to the degree of compactness for each sample (bulk density and hydraulic conductivity). To generate a visual display of variance at the sub- field scale, mean values for bulk density (*Figure 4.4*) and hydraulic conductivity (*Figure 4.5*) after compaction at each of the different stress states were plotted, assuming the 3 specific moisture contents for each monitoring point as replicates. Analysis of the compacted bulk density populations reveals the P- value (probability of observing a result (F-critical) as large as the one which is observed in the experiment (F)) for each field is less than the significance level ($\alpha = 0.05$), this infers the differences between some of the means are statistically significant (Tarlow, 2016).

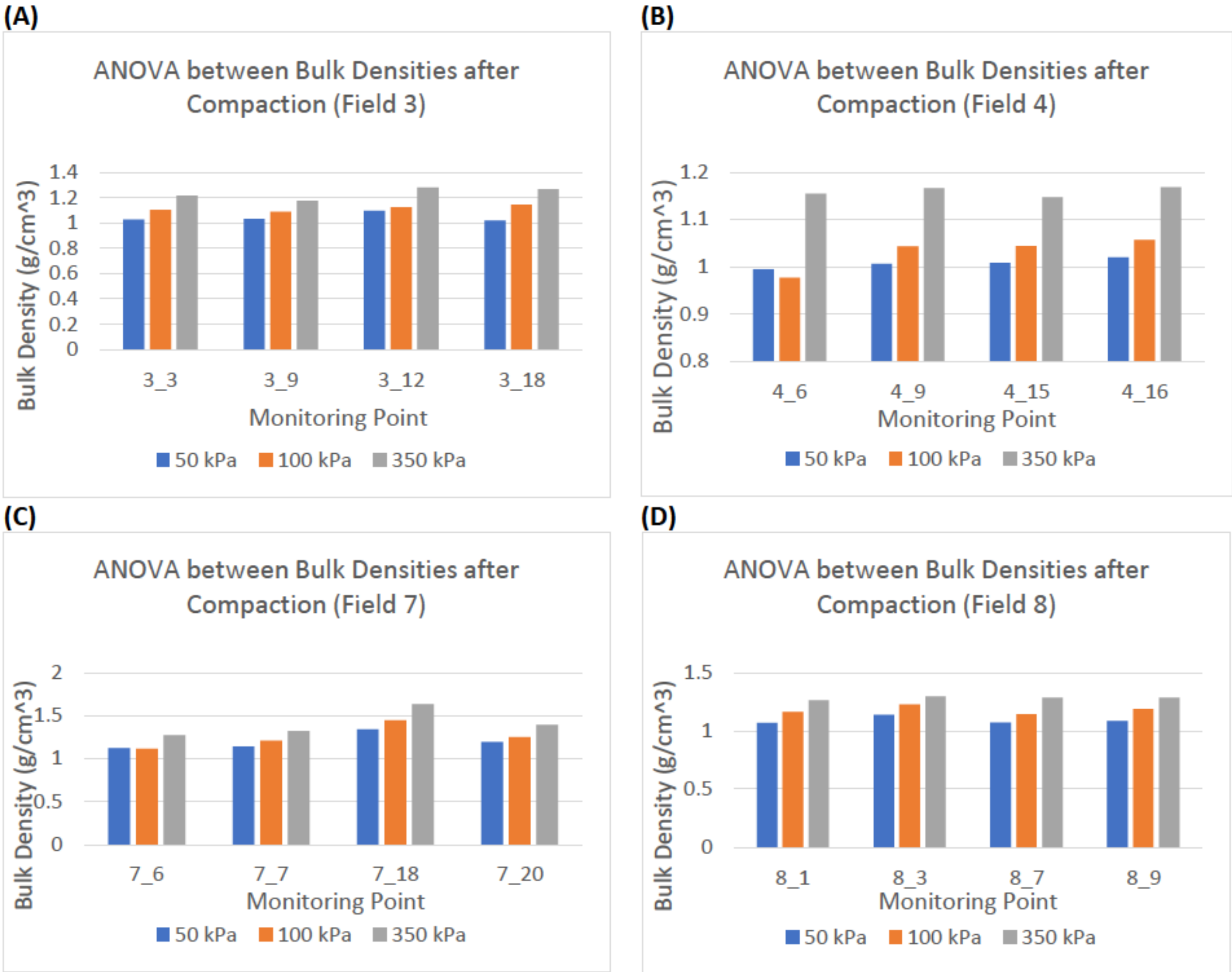

Figure 4.4 *Analysis of sub- field variance between mean bulk densities after compaction at 3 specific moisture contents for each stress state (A) ANOVA at DALBY- Steve McVeigh Field 3, (B) ANOVA at DALBY- Shawn Fresser Field 4, (C) ANOVA at TALWOOD- Ben Turner Field 7, and (D) ANOVA at TALWOOD- Tom Seerey Field 8*

Analysis of the compacted hydraulic conductivity populations reveals the P- value for is greater than the significance level ($\alpha = 0.05$) for each field, except Site 4, (*Figure 4.5- (B)*). This infers the differences between some of the means are statistically significant for this site only (Tarlow, 2016). The differences between the means at Sites 3, 7 & 8 are not statistically significant. It is important to note that although variance in both physical and chemical properties is evident between monitoring points, no consistent relationships are observed on the sub-field scale.

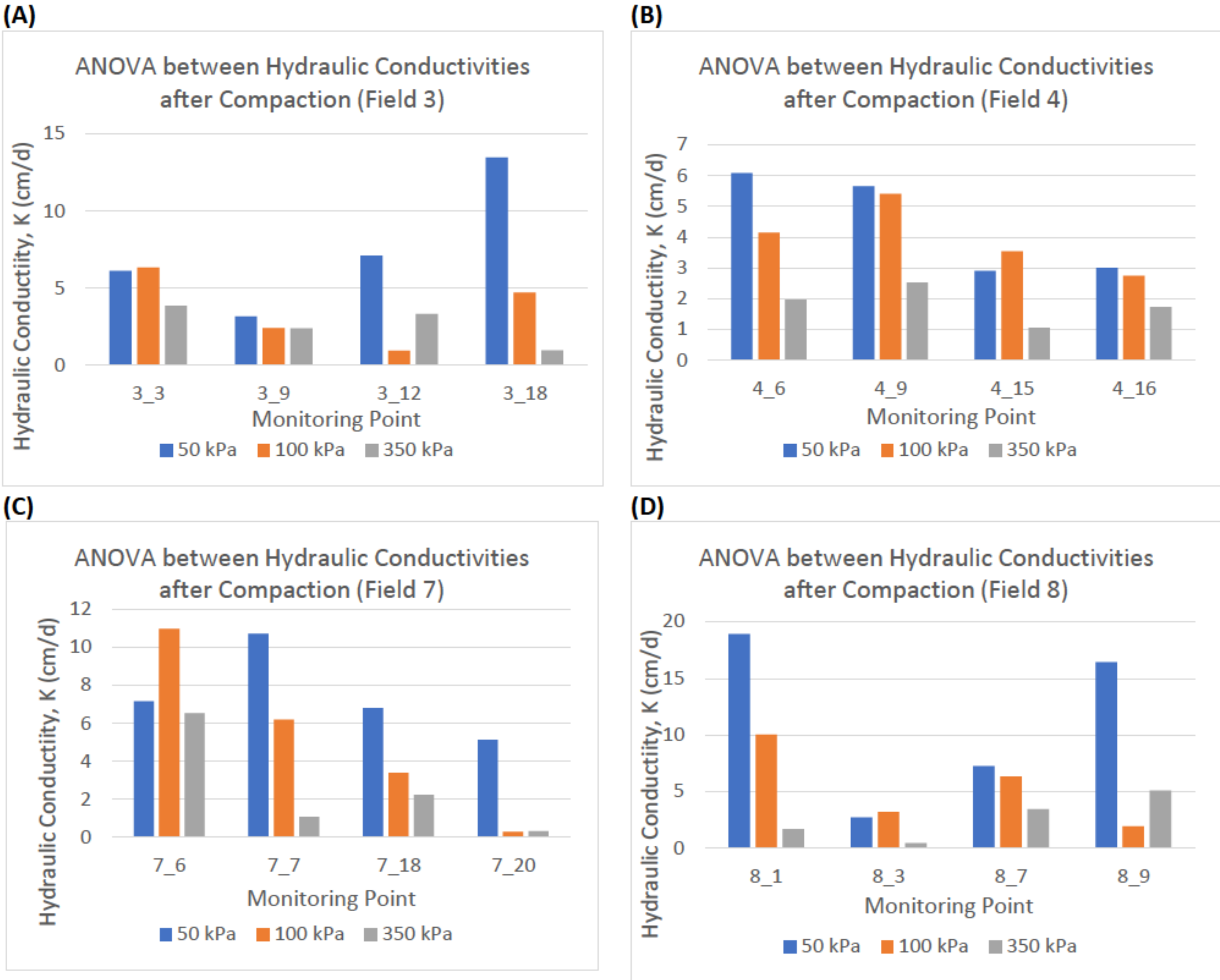

Figure 4.5 *Analysis of sub- field variance between mean hydraulic conductivities after compaction at 3 specific moisture contents for each stress state (A) ANOVA at DALBY- Steve McVeigh Field 3, (B) ANOVA at DALBY- Shawn Fresser Field 4, (C) ANOVA at TALWOOD- Ben Turner Field 7, and (D) ANOVA at TALWOOD- Tom Seerey Field 8. Where absent data points are substituted with local means (Shaw & Mitchell-Olds, 1993).*

Additionally, an ANOVA between all 4 fields was conducted to identify geographic relationships. Mean values for bulk density (*Figure 4.6- (A)*) and hydraulic conductivity (*Figure 4.6- (B)*) after compaction at each soil's plastic limit at each of the different stress states were plotted, assuming the 4 different monitoring points within each field as replicates. Analysis of both the compacted bulk density and hydraulic conductivity populations reveals the P- value for both parameters is less than the significance level ($\alpha = 0.05$), this infers the differences between some of the means are statistically significant (Tarlow, 2016).

(A) (B)

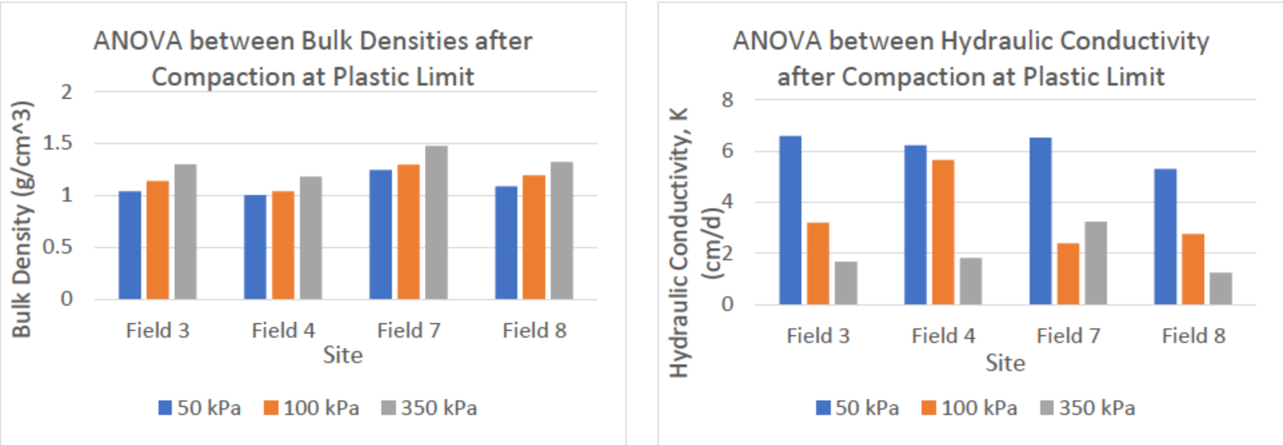

Figure 4.6 *Analysis of variance in degree of compaction between fields (A) ANOVA between mean bulk densities after compaction at each soil's plastic limit for each stress state, (B) ANOVA between mean hydraulic conductivities after compaction at each soil's plastic limit for each stress state, where absent data points are substituted with local means (Shaw & Mitchell-Olds, 1993).*

4.5.2 Outliers

The innovative nature of experimental procedures implemented in this study require a thorough analysis of the results produced to ensure validity. In particular, it was observed that a number of infiltration tests were compromised by insufficient hydraulic contact. This occurred predominantly with the natural swelling behavior of heavy clay soils and occasionally with the incorrect setup of apparatus (human error). As such, the processed results were analysed again and outliers were detected as data points which were 1.5 times greater than the interquartile range (IQR) outside of the first or third quartiles as recommended by (Hamilton, 1990). This inferred the removal of four separate data points, all of which were relatively unrealistic and significantly beyond the IQR of the first or third quartiles (hydraulic conductivity, K = 49.0 cm/d after simulation of machine loading). All data sets for uniaxial compression and spatial variance were apprehensive and analysed in the results section.

4.5.3 Sensitivity Analysis

A sensitivity analysis was conducted for the applied loading in the uniaxial compression procedure. It was observed during this method that a minor delay in instrument communication and human error meant that the target applied load was often exceeded (by less than 5%), when simulating compaction. This was particularly experienced for samples which received an implied stress state of 350 kPa. As the applied load of 2040 N exceeds the precompression strength of the soil and soil failure occurs, the rate of deflection remains constant as the rate of applied load increases exponentially, as seen in the figure below. As a result of this, the target load was often missed, (exceeded).

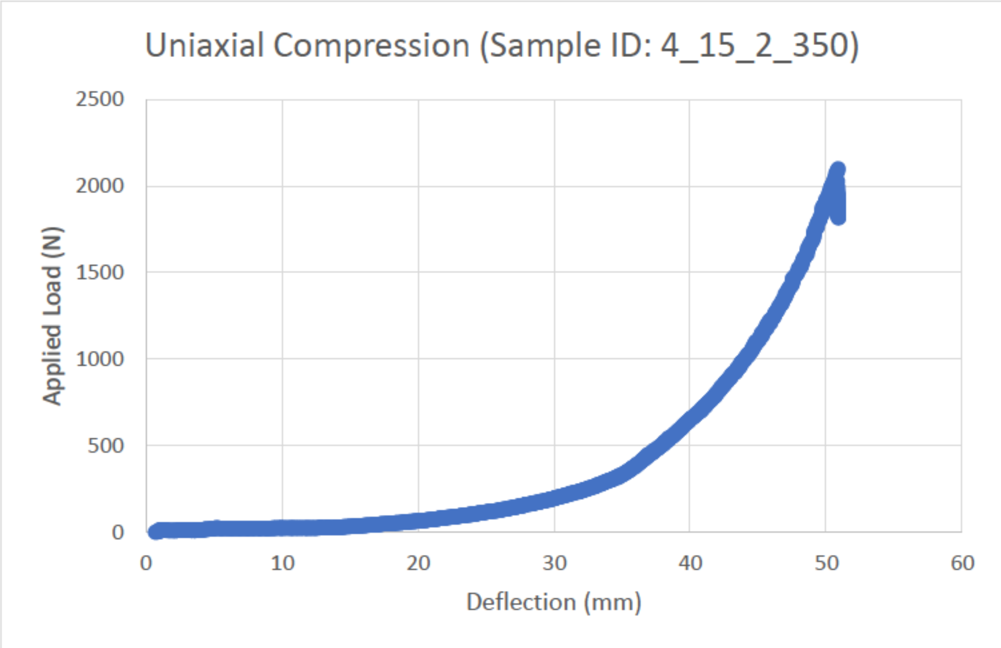

***Figure 4.7** Plot comparing applied load versus sample deflection produced from the uniaxial compression test for SAMPLE: 4_15, moistened to the soils specific plastic limit and load applied to simulate a surface stress state of 350 kPa.*

Therefore, a sensitivity analysis was conducted to determine the significance of this error and the resultant effect on the dependent variables. For a trial sample, prepared with the same procedure as those used in the study, the difference in deflection was analysed as the implied load was exceeded by 10% for each of the chosen stress states. The results are tabulated below.

***Table 4.5** Sensitivity analysis on sample deflection with regards to applied load.*

	Target Load (2040 N)	Exceeded Load, 10% (2244 N)	Degree of Difference (%)
Deflection (mm)	57.536	58.084	0.943

Accuracy of recorded deflection results is critical as it determines the volume of each sample used in soil bulk density calculations. Despite this, a sensitivity analysis of 10% exceedance is an exaggeration of what would actually be observed in procedure and yet the degree of difference remains below 1%. It can hence be concluded that the applied load has a proportionally insignificant effect on deflection in this experimental procedure and these errors can be ignored in results analysis.

5. DISCUSSION

5.1 FACTORS CONTRIBUTING TO COMPACTION RISK

The contents of this section convey an investigation of the interaction between soil constraints and conclusions drawn from the results. Furthermore, a thorough analysis of the findings provides sufficient evidence to quantify the extent of the soil compaction as affected by spatial variability at the sub-field scale with respect to soil type and soil constraint changes.

Prior to completion, this study presumed there would not be any significant variability in soil compaction impact for a given moisture content spatially within a given soil type. The outcomes suggest this is not entirely true. A statistical analysis of the results quantifying the extent of compaction at a range of stress states computed a degree of variance at the sub- field scale for each site. More specifically, sample bulk densities recorded for all fields after compaction exhibited statistically significant variance. This was also observed when analysing the variance of sample hydraulic conductivities after compaction at Field 4. In contrast, the analysis suggested that despite the spatial occurrence of varying soil constraints in Fields 3, 7 & 8, significant variability was not observed in hydraulic conductivities after compaction, supporting the alternate hypothesis. Additionally, a statistical analysis of the four sites investigated identified significant variance in mean values for bulk density and hydraulic conductivity after compaction at each soil's plastic limit, suggesting the absence of geographic relationships. Despite observed sub- field variance in the degree of compactness after simulation of differing stress states, the results do not provide evidence of relationships between soil constraint variance and susceptibility to compaction.

It was found in the investigation that as all soils were loaded with a magnitude of mechanical stress to simulate machine traffic (350kPa), bulk densities approach or exceed the literature recommended value for plant growth in a compressed clay soil. This suggests that in contrast to the findings from the statistical analysis, the degree of variance at the sub- field scale is not practically significant, providing evidence against the null hypothesis. When subjected to this measure of pressure, soil precompression stress is exceeded and critical failure occurs. In this condition, the soil pore space is substantially reduced, minimising potential for plant root growth and inhibiting soil infiltrative properties. Furthermore, after degradation to this extent, very little rebound, (increase in soil volume as a consequence of decrease in effective stress) is experienced and the compaction is deemed irreversible. The severity of this is most significant when soil is compressed at the OMC. The results indicated this moisture content is generally slightly below the soil's plastic limit.

By measuring the changes in the hydraulic conductivity, as soil is compacted under differing conditions, assumptions about the fluctuations in water penetrative resistance of the field can be made. The extent of soil compaction in this study is quantified by the calculated values of Hydraulic conductivity, derived from measured cumulative infiltration for each sample after compression. When considering these results, it is important to acknowledge several parameters. The infiltrometers used in the study had a diameter of 50mm, meaning that the majority of the infiltration within the 86.2mm diameter sample is downwards flow, however horizontal flow should also be considered. Ultimately, a graphical display of the findings reveals the majority of curves follow a similar trend, particularly after simulated machine loading. This reinforces the statistical analysis of these properties suggesting that the variance in compaction extent is not practically significant on the sub- field scale.

A spatial analysis of the soil compaction vulnerability reveals the extent of compaction generally does vary significantly throughout the field (selected monitoring points) when compared across a range of moisture contents and stress states. However, values are still low enough to limit plant available water, indicating compaction severity to be the overriding factor. Furthermore, no trends are evident in regards to a certain soil maintaining a greater hydraulic conductivity across all tested stress states. Additionally, variance reduces as moisture content and applied load is increased as soils are more susceptible to compaction at these conditions. This relationship supports the experimental hypothesis that sub-field constraint variability has a minimal effect on the soil's susceptibility to compaction. However, a lack of evidence infers this alternate hypothesis is only partially correct and should not be accepted.

5.2 Consequences of Compaction Extent

It can be concluded from the procedures that irreversible compaction is detrimental and largely inevitable with the traverse of modern machinery. This statement can be fortified by work published on quantifying compaction in clay soils, (*Indicator Test Function USDANaturalResourcesConservationService - NRCS*, 2022). This study observed that bulk densities above $1.4\ \mathrm{g/cm^3}$ in clay soils can be classed as compacted, and at this density, plant root growth is restricted, forcing the requirement of conservation practices to mediate effects.

Literature on quantifying the hydraulic conductivity of soils after compaction is limited. (Nielsen et al., 1961) states the hydraulic conductivity of a soil in its proximal benchmark condition can range from about 30 m/d for a silty clay loam to about 5 cm/d for a clay. Disturbance can reduce this value to approximately 2 cm/d for silt and clay soils. In addition to this, (Kim et al., 2010) identified relationships between soil bulk density and the saturated hydraulic conductivity. It was demonstrated that increasing the soil bulk density by 8% results in a 70% reduction of saturated hydraulic conductivity. This relationship can be described as an exponential decline in hydraulic conductivity as soil porosity is reduced (Awedat et al., 2021). This is backed by work on similarly textured soil by (Awedat et al., 2012) which reports a 20% increase in bulk density infers an 84% reduction in the saturated hydraulic conductivity of the soil. This supports results revealed in this study depicting the hydraulic conductivity of each soil approaching zero as moisture content increases and enhances the severity of machine simulated compaction in terms of bulk density. Plant available water content of soil in this condition would be limited and crop establishment restricted.

5.3 Considerations for Further Work

Ultimately, this investigation failed to provide sufficient evidence to completely reject the null hypothesis. However, this provides a useful insight for developing current practices and designing experiments to achieve more comprehensive outcomes. A reflection of the methods executed in this study reveals a number of techniques which could be improved and areas which require further investigation to draw conclusive results. The dataset presented for Atterberg limits in this study were marginally lower than expected for Vertosols in this region. Possible data error here may originate from a several causes. Despite a rigorous procedure and 4-point Casagrande method to determine liquid limits, assumptions made in this technique are generally subjective and could be improved with the supervision of a superior. Furthermore, it was observed that equilibration in preparation for uniaxial compression testing was insufficient for several samples, particularly at low moisture contents. This is likely inhibited by dispersive properties of the soil. In addition to this, as mentioned above, it is suspected that some inaccuracies are present in the hydraulic conductivity data as a result of disturbance to the infiltrometer and hence a break in hydraulic contact during the procedure. This may be responsible for the degree of uniformity in results.

Several areas of this methodology should be revised to enhance the dimension of further work completed in this field. This study focused on only soil sampled from the top-soil region of the soil profile. A more thorough assessment of the compaction extent could be made with the analysis of soil degradation by compaction with depth. By additional sampling to represent the sub-soil (>40cm depth) regions of the profile, a more conclusive assessment of severity may be made. Furthermore, developing uniaxial compression curves for only three tested moisture contents provides a limited display. A more comprehensive assessment of OMC would be achieved by completing replicates for further samples at varying moisture contents.

6. Conclusion

This section conveys the outcomes regarding the effects of spatial variability of soil constraints within a soil type at the sub-field level in regards to the magnitude of mechanical stress that is implemented by machine traffic. Additionally, several recommendations to be considered by land holders for future management practices are made based on the evidence presented in this study. An industry reluctance to switch from random traffic or semi-controlled traffic to a true controlled traffic system can be attributed to several justifications. Perhaps the most predominant is the misconception of the factors affecting a soils vulnerability to compaction. This investigation was conducted to highlight considerations for best soil management, with regards to variance in geolocation, soil condition and constraining factors as a result of physical and chemical properties.

It is apparent that the samples evaluated in this study experienced substantial extents of soil compaction, measured as an increase in bulk density and hydraulic reduction, particularly after procedure to mimic machine traffic. This result is expected given the simulated axle loads inferring a stress state of 350 kPa to the soil surface (Keller et al., 2007). Furthermore, it was found that this phenomenon is often enhanced and generally irreversible when compaction occurs at soil moisture content near or above the plastic limit. Hence, the avoidance of machine wheeling at these field conditions is strongly recommended to preserve the soil resource.

The constraint diagnosis of soils from each site revealed considerable differences in both the soil physical and chemical properties when considering the entire profile. This is likely to inhibit plant growth in some areas and impose variance in crop performance throughout the field, motivating interest in amelioration techniques. Whilst no direct relationships can be drawn between soil pedological factors and constraints, the investigation observed significant variance in compaction parameters at the subfield scale, at a rage of sites, thus, the null hypothesis should not be rejected. However, these values for the degree of compactness indicate plant growth will be restricted under these conditions. Inferring the key message being the overriding effect of stress on compaction and hydraulic reduction despite sub-field variability. This suggests soil compaction should be first addressed, then avoided prior to soil structural amelioration efforts. Ultimately, the effect of spatial constraint variability on a soil’s susceptibility to compaction remains largely unknown. Despite this, the significant expense of true controlled traffic can be justified by the unequivocal evidence that the extent of compaction will be the dominant contributor to soil degradation.

7. REFERENCES

Alakukku, L. (1999). Subsoil compaction due to wheel traffic. *Agricultural and Food Science*, *8*(4-5), 333-351.

Alaoui, A., & Diserens, E. (2018). Mapping soil compaction–A review. *Current opinion in environmental science & health*, *5*, 60-66.

Ankeny, M. D., Kaspar, T. C., & Horton, R. (1990). Characterization of tillage and traffic effects on unconfined infiltration measurements. *Soil Science Society of America Journal*, *54*(3), 837-840.

Ansorge, D., & Godwin, R. (2007). The effect of tyres and a rubber track at high axle loads on soil compaction, Part 1: Single axle-studies. *Biosystems Engineering*, *98*(1), 115-126.

Antille, D. L., Ansorge, D., Dresser, M. L., & Godwin, R. J. (2013). Soil displacement and soil bulk density changes as affected by tire size. *Transactions of the ASABE*, *56*(5), 1683-1693.

Antille, D. L., Bennett, J. M., & Jensen, T. A. (2016). Soil compaction and controlled traffic considerations in Australian cotton-farming systems. *Crop and Pasture Science*, *67*(1), 1-28.

Arvidsson, J. (1998). Influence of soil texture and organic matter content on bulk density, air content, compression index and crop yield in field and laboratory compression experiments. *Soil and Tillage Research*, *49*(1-2), 159-170.

Australia's official weather forecasts & weather radar - Bureau of Meteorology. (2022). Retrieved 12 October from http://www.bom.gov.au/

Awedat, A., Raine, S., Bennett, J. M., & Misra, R. (2012). Influence of porosity and permeate suspended clay concentration on clay entrainment within a red ferrosol. Proceedings of the 5th Joint Australian and New Zealand Soil Science Conference (SSA 2012),

Awedat, A. M., Zhu, Y., Bennett, J. M., & Raine, S. R. (2021). The impact of clay dispersion and migration on soil hydraulic conductivity and pore networks. *Geoderma*, *404*, 115297.

Barik, K., Aksakal, E. L., Islam, K. R., Sari, S., & Angin, I. (2014). Spatial variability in soil compaction properties associated with field traffic operations. *Catena*, *120*, 122-133.

Bennett, J., Woodhouse, N. P., Keller, T., Jensen, T. A., & Antille, D. L. (2015). Advances in cotton harvesting technology: a review and implications for the John Deere Round Baler Cotton Picker. *Journal of Cotton Science*, *19*(2), 225-249.

Bennett, J. M. (2022). Decision framework for profitable soil constraint management.

Bennett, J. M., Greene, R., Murphy, B., Hocking, P., & Tongway, D. (2014). Influence of lime and gypsum on long-term rehabilitation of a Red Sodosol, in a semi-arid environment of New South Wales. *Soil Research*, *52*(2), 120-128.

Bennett, J. M., Jensen, T., Antille, D., & Baillie, C. (2016). An impact assessment framework for harvesting technologies in cotton: management considerations for the John Deere 7760.

Bennett, J. M., Roberton, S., Marchuk, S., Woodhouse, N., Antille, D., Jensen, T., & Keller, T. (2019). The soil structural cost of traffic from heavy machinery in Vertisols. *Soil and Tillage Research*, *185*, 85-93.

Bennett, J. M., Roberton, S. D., Jensen, T. A., Antille, D. L., & Hall, J. (2017). A comparative study of conventional and controlled traffic in irrigated cotton: I. Heavy machinery impact on the soil resource. *Soil and Tillage Research*, *168*, 143-154.

Bennett, J. W. (2017). *The ecological transition: cultural anthropology and human adaptation*. Routledge.

Berisso, F., Schjønning, P., Keller, T., Lamandé, M., Etana, A., De Jonge, L., Iversen, B., Arvidsson, J., & Forkman, J. (2012). Persistent effects of subsoil compaction on pore size distribution and gas transport in a loamy soil. *Soil and Tillage Research*, *122*, 42-51.

Biggs, A., Harms, B., & Payne, J. (2010). Alkaline sodic soils of the Yelarbon area, Australia. Proceedings of the 19th World Congress of Soil Science: Soil solutions for a changing world, Brisbane, Australia, 1-6 August 2010. Division Symposium 2.2 Management of landscapes for the future,

Blake, G. R., & Hartge, K. (1986). Particle density. *Methods of soil analysis: Part 1 physical and mineralogical methods*, *5*, 377-382.

Boussinesq, J. (1885). *Application des potentiels à l'étude de l'équilibre et du mouvement des solides élastiques: principalement au calcul des déformations et des pressions que produisent, dans ces solides, des efforts quelconques exercés sur une petite partie de leur surface ou de leur intérieur: mémoire suivi de notes étendues sur divers points de physique, mathematique et d'analyse* (Vol. 4). Gauthier-Villars.

Braunack, M., & Johnston, D. (2014). Changes in soil cone resistance due to cotton picker traffic during harvest on Australian cotton soils. *Soil and Tillage Research*, *140*, 29-39.

Bui, E. N., Loughhead, A., & Corner, R. (1999). Extracting soil-landscape rules from previous soil surveys. *Soil Research*, *37*(3), 495-508.

Castrignano, A., Maiorana, M., Fornaro, F., & Lopez, N. (2002). 3D spatial variability of soil strength and its change over time in a durum wheat field in Southern Italy. *Soil and Tillage Research*, *65*(1), 95-108.

Chamen, W. T., Moxey, A. P., Towers, W., Balana, B., & Hallett, P. D. (2015). Mitigating arable soil compaction: A review and analysis of available cost and benefit data. *Soil and Tillage Research*, *146*, 10-25.

Chancellor, W., Schmidt, R., & Soehne, W. (1962). Laboratory measurement of soil compaction and plastic flow.

Chinn, C., & Pillai, U. (2008). Self-repair of compacted Vertisols from central Queensland, Australia. *Geoderma*, *144*(3-4), 491-501.

Chyba, J., Kroulík, M., Krištof, K., Misiewicz, P., & Chaney, K. (2014). Influence of soil compaction by farm machinery and livestock on water infiltration rate on grassland. *Agronomy Research*, *12*(1), 59-64.

CSIRO. (2022). Retrieved 12 October from https://www.csiro.au/en/

Dang, Y. (2022). Soil constraints to crop production: an overview.

Daniells, I., Larsen, D., McKenzie, D., & Anthony, D. (1996). SOILpak: a successful decision support system for managing the structure of Vertisols under irrigated cotton. *Soil Research*, *34*(6), 879-889.

Dawidowski, J., & Lerink, P. (1990). Laboratory simulation of the effects of traffic during seedbed preparation on soil physical properties using a quick uni-axial compression test. *Soil and Tillage Research*, *17*(1-2), 31-45.

Défossez, P., & Richard, G. (2002). Models of soil compaction due to traffic and their evaluation. *Soil and Tillage Research*, *67*(1), 41-64.

Edling, P., & Fergedal, L. (1972). Model experiments on soil compaction 1968-69. *Swedish Univ. Agric. Sci., Uppsala, Div. Soil Management, Report*, *31*, 71.

Fröhlich, O. (1934). Das elastische Verhalten der Böden. In *Druckverteilung im Baugrunde* (pp. 86-108). Springer.

Gens, A., & Potts, D. (1988). Critical state models in computational geomechanics. *Engineering Computations*.

Graves, A., Morris, J., Deeks, L., Rickson, R., Kibblewhite, M., Harris, J., Farewell, T., & Truckle, I. (2015). The total costs of soil degradation in England and Wales. *Ecological Economics*, *119*, 399-413.

Gysi, M., Ott, A., & Flühler, H. (1999). Influence of single passes with high wheel load on a structured, unploughed sandy loam soil. *Soil and Tillage Research*, *52*(3-4), 141-151.

Håkansson, I. (1990). A method for characterizing the state of compactness of the plough layer. *Soil and Tillage Research*, *16*(1-2), 105-120.

Håkansson, I., Voorhees, W. B., & Riley, H. (1988). Vehicle and wheel factors influencing soil compaction and crop response in different traffic regimes. *Soil and Tillage Research*, *11*(3-4), 239-282.

Hamilton, J. D. (1990). Analysis of time series subject to changes in regime. *Journal of econometrics*, *45*(1-2), 39-70.

Hamza, M., Al-Adawi, S., & Al-Hinai, K. (2011). Effect of combined soil water and external load on soil compaction. *Soil Research*, *49*(2), 135-142.

Hazelton, P., & Murphy, B. (2016). *Interpreting soil test results: What do all the numbers mean?* CSIRO publishing.

Horn, R., Domżżał, H., Słowińska-Jurkiewicz, A., & Van Ouwerkerk, C. (1995). Soil compaction processes and their effects on the structure of arable soils and the environment. *Soil and Tillage Research*, *35*(1-2), 23-36.

Horn, R., & Fleige, H. (2003). A method for assessing the impact of load on mechanical stability and on physical properties of soils. *Soil and Tillage Research*, *73*(1-2), 89-99.

Horn, R., Way, T., & Rostek, J. (2003). Effect of repeated tractor wheeling on stress/strain properties and consequences on physical properties in structured arable soils. *Soil and Tillage Research*, *73*(1-2), 101-106.

Horton, R. E. (1933). The role of infiltration in the hydrologic cycle. *Eos, Transactions American Geophysical Union*, *14*(1), 446-460.

Idso, S. B., Reginato, R. J., & Jackson, R. D. (1977). An equation for potential evaporation from soil, water, and crop surfaces adaptable to use by remote sensing. *Geophysical research letters*, *4*(5), 187-188.

Indicator Test Function USDANaturalResourcesConservationService - NRCS. (2022). Retrieved 12 October from https://www.nrcs.usda.gov/Internet/FSE_DOCUMENTS/nrcs142p2_053256.pdf

Ishaq, M., Hassan, A., Saeed, M., Ibrahim, M., & Lal, R. (2001). Subsoil compaction effects on crops in Punjab, Pakistan: I. Soil physical properties and crop yield. *Soil and Tillage Research*, *59*(1-2), 57-65.

Jackson, T., Chang, A., & Schmugge, T. (1981). Active microwave measurements for estimating soil moisture in Oklahoma. Rainbow 80; Fall Technical Meeting,

Jamali, H., Nachimuthu, G., Palmer, B., Hodgson, D., Hundt, A., Nunn, C., & Braunack, M. (2021). Soil compaction in a new light: Know the cost of doing nothing–A cotton case study. *Soil and Tillage Research*, *213*, 105158.

Johnson, C., & Burt, E. (1990). A method of predicting soil stress state under tires. *Transactions of the ASAE*, *33*(3), 713-0717.

Kadlec, V., Holubík, O., Prochazkova, E., Urbanova, J., & Tippl, M. (2012). Soil organic carbon dynamics and its influence on the soil erodibility factor. *Soil and Water Research*, *7*(3), 97-108.

Kargas, G., Persson, M., Kanelis, G., Markopoulou, I., & Kerkides, P. (2017). Prediction of soil solution electrical conductivity by the permittivity corrected linear model using a dielectric sensor. *Journal of Irrigation and Drainage Engineering*, *143*(8), 04017030.

Keller, T., Défossez, P., Weisskopf, P., Arvidsson, J., & Richard, G. (2007). SoilFlex: A model for prediction of soil stresses and soil compaction due to agricultural field traffic including a synthesis of analytical approaches. *Soil and Tillage Research*, *93*(2), 391-411.

Keller, T., Sandin, M., Colombi, T., Horn, R., & Or, D. (2019). Historical increase in agricultural machinery weights enhanced soil stress levels and adversely affected soil functioning. *Soil and Tillage Research*, *194*, 104293.

Kim, H., Anderson, S., Motavalli, P., & Gantzer, C. (2010). Compaction effects on soil macropore geometry and related parameters for an arable field. *Geoderma*, *160*(2), 244-251.

Kingsley, J., Egerer, M., Nuttman, S., Keniger, L., Pettitt, P., Frantzeskaki, N., Gray, T., Ossola, A., Lin, B., & Bailey, A. (2021). Urban agriculture as a nature-based solution to address socio-ecological challenges in Australian cities. *Urban Forestry & Urban Greening*, *60*, 127059.

Kingwell, R., & Fuchsbichler, A. (2011). The whole-farm benefits of controlled traffic farming: An Australian appraisal. *Agricultural Systems*, *104*(7), 513-521.

Kirby, J. (1991). Critical-state soil mechanics parameters and their variation for Vertisols in eastern Australia. *Journal of Soil Science*, *42*(3), 487-499.

Koolen, A., Lerink, P., Kurstjens, D., Van den Akker, J., & Arts, W. (1992). Prediction of aspects of soil-wheel systems. *Soil and Tillage Research*, *24*(4), 381-396.

Koolen, A. J., & Kuipers, H. (1983). Mechanical behavior of soil elements. In *Agricultural Soil Mechanics* (pp. 9-90). Springer.

Lai, J., & Ren, L. (2007). Assessing the size dependency of measured hydraulic conductivity using double-ring infiltrometers and numerical simulation. *Soil Science Society of America Journal*, *71*(6), 1667-1675.

Latorre, B., Moret-Fernández, D., & Peña, C. (2013). Estimate of soil hydraulic properties from disc infiltrometer three-dimensional infiltration curve: theoretical analysis and field applicability. *Procedia Environmental Sciences*, *19*, 580-589.

Lebert, M., & Horn, R. (1991). A method to predict the mechanical strength of agricultural soils. *Soil and Tillage Research*, *19*(2-3), 275-286.

Lili, M., Bralts, V. F., Yinghua, P., Han, L., & Tingwu, L. (2008). Methods for measuring soil infiltration: State of the art. *International Journal of Agricultural and Biological Engineering*, *1*(1), 22-30.

Lipiec, J., & Hatano, R. (2003). Quantification of compaction effects on soil physical properties and crop growth. *Geoderma*, *116*(1-2), 107-136.

Madsen, M. D., & Chandler, D. G. (2007). Automation and use of mini disk infiltrometers. *Soil Science Society of America Journal*, *71*(5), 1469-1472.

McBratney, A. B., Santos, M. M., & Minasny, B. (2003). On digital soil mapping. *Geoderma*, *117*(1-2), 3-52.

METER. (2022). Retrieved 11 October from https://www.metergroup.com/

Nawaz, M. F., Bourrie, G., & Trolard, F. (2013). Soil compaction impact and modelling. A review. *Agronomy for sustainable development*, *33*(2), 291-309.

Nielsen, D. R., Kirkham, D., & Van Wijk, W. (1961). Diffusion equation calculations of field soil water infiltration profiles. *Soil Science Society of America Journal*, *25*(3), 165-168.

O'sullivan, M., Henshall, J., & Dickson, J. (1999). A simplified method for estimating soil compaction. *Soil and Tillage Research*, *49*(4), 325-335.

Page, K., Dalal, R., Wehr, J., Dang, Y., Kopittke, P., Kirchhof, G., Fujinuma, R., & Menzies, N. (2018). Management of the major chemical soil constraints affecting yields in the grain growing region of Queensland and New South Wales, Australia–a review. *Soil Research*, *56*(8), 765-779.

Pillai, U., & McGarry, D. (1999). Structure repair of a compacted Vertisol with wet-dry cycles and crops. *Soil Science Society of America Journal*, *63*(1), 201-210.

Pinzón-Gómez, L. P., Álvarez-Herrera, J. G., & Mesa-Amezquita, A. (2016). Study of the spatial variability of moisture and compaction in soils with different plant covers. *Agronomía Colombiana*, *34*(3), 355-363.

Radford, B., Yule, D., McGarry, D., & Playford, C. (2007). Amelioration of soil compaction can take 5 years on a Vertisol under no till in the semi-arid subtropics. *Soil and Tillage Research*, *97*(2), 249-255.

Raghavan, G., McKyes, E., & Chassé, M. (1977). Effect of wheel slip on soil compaction. *Journal of Agricultural Engineering Research*, *22*(1), 79-83.

Rankine, W. J. M. (1857). On the stability of loose earth. *Phil. Trans. R. Soc.*(147), 9-27.

Reichle, R. H., De Lannoy, G. J., Liu, Q., Colliander, A., Conaty, A., Jackson, T., Kimball, J., & Koster, R. D. (2015). *Soil moisture active passive (SMAP) project assessment report for the beta-release L4_SM data product*. National Aeronautics and Space Administration, Goddard Space Flight Center.

Roscoe, K. H. (1968). On the generalized stress-strain behaviour of 'wet' clay. *Engineering Plasticity*, 535-609.

Rosetta. (2022). Retrieved October 12 from https://www.handbook60.org/rosetta/

RStudio Team. (2015). http://www.rstudio.com/

Shaw, R., Brebber, L., Ahern, C., & Weinand, M. (1994). A review of sodicity and sodic soil behavior in Queensland. *Soil Research*, *32*(2), 143-172.

Shaw, R. G., & Mitchell-Olds, T. (1993). ANOVA for unbalanced data: an overview. *Ecology*, *74*(6), 1638-1645.

Smith, P., Smith, J., Powlson, D., McGill, W., Arah, J., Chertov, O., Coleman, K., Franko, U., Frolking, S., & Jenkinson, D. (1997). A comparison of the performance of nine soil organic matter models using datasets from seven long-term experiments. *Geoderma*, *81*(1-2), 153-225.

Soane, B., & Van Ouwerkerk, C. (1994). Soil compaction problems in world agriculture. In *Developments in agricultural engineering* (Vol. 11, pp. 1-21). Elsevier.

Söhne, v. W. (1953). Druckverteilung im ackerboden und verformbarkeit des ackerbodens. *Kolloid-Zeitschrift*, *131*(2), 89-96.

Steffan, R. J., & Schaefer, C. E. (2016). Current and future bioremediation applications: bioremediation from a practical and regulatory perspective. In *Organohalide-respiring bacteria* (pp. 517-540). Springer.

Suzuki, L., Reichert, J., & Reinert, D. (2013). Degree of compactness, soil physical properties and yield of soybean in six soils under no-tillage. *Soil Research*, *51*(4), 311-321.

Tarlow, K. R. (2016). Teaching principles of inference with ANOVA. *Teaching Statistics*, *38*(1), 16-21.

Tilse, M. J., Bishop, T. F., Triantafilis, J., & Filippi, P. (2022). Mapping the impact of subsoil constraints on soil available water capacity and potential crop yield. *Crop and Pasture Science*, *73*(6), 636-651.

Tullberg, J., Yule, D., & McGarry, D. (2007). Controlled traffic farming—from research to adoption in Australia. *Soil and Tillage Research*, *97*(2), 272-281.

Virmani, S., Sahrawat, K., & Burford, J. (1982). Physical and chemical properties of Vertisols and their management.

Walsh, P. (2002). New method yields a worm's eye view. *Farming Ahead*(132), 16-18.

Wander, M. M., Walter, G. L., Nissen, T. M., Bollero, G. A., Andrews, S. S., & Cavanaugh-Grant, D. A. (2002). Soil quality: science and process. *Agronomy Journal*, *94*(1), 23-32.

Wösten, J., Lilly, A., Nemes, A., & Le Bas, C. (1999). Development and use of a database of hydraulic properties of European soils. *Geoderma*, *90*(3-4), 169-185.

Yao, Y.-P., & Sun, D. A. (2000). Application of Lade's criterion to Cam-clay model. *Journal of engineering mechanics*, *126*(1), 112-119.

Zhang, R. (1997). Determination of soil sorptivity and hydraulic conductivity from the disk infiltrometer. *Soil Science Society of America Journal*, *61*(4), 1024-1030.

Zimmermann, B., Elsenbeer, H., & De Moraes, J. M. (2006). The influence of land-use changes on soil hydraulic properties: Implications for runoff generation. *Forest ecology and management*, *222*(1-3), 29-38.

8. APPENDICES

8.1 APPENDIX A

Project Specification

ENG4111/4112 Research Project

Project Specification

For: Danny O'Connor- 0061117934

Title: Soil compaction dependence on sub-field spatial soil constraint variability

Major: Agricultural

Supervisors: John Bennet, Stirling Roberton

Enrollment: ENG4111 – EXT S1, 2021

ENG4112 – EXT S2, 2021

Project Aim: Quantify soil compaction extent as affected by spatial variability at the sub-field scale with respect to soil type and soil constraint changes

Programme: Version 1, 10th March 2021

1. Select a minimum of four sites (one field at each site), at GRDC recognised sites in the darling downs and greater western NSW regions.
2. Spatially diagnose the soil type and soil constraint variability at the sub-field scale.
3. Using pedometric techniques, select representative monitoring points within the field from which to sample soil for compaction experimentation.
4. Determine sufficient parameters and procedures for conducting soil mechanics tests and source required equipment.
5. Using a uniaxial compression test, determine the change in density of the soil at a range of moisture contents and stress states for each monitoring location. Depending on time and availability of equipment, these tests may be repeated to ensure reliability.
6. From the compressed sample, determine the change in saturated hydraulic conductivity.
7. Using the soil type and constraint diagnosis, investigate the interaction between constraints, depth, stress state and moisture content on the reduction in soil pore geometry as inferred from saturated hydraulic conductivity.
8. Quantify the extent of the soil compaction as affected by spatial variability at the sub-field scale with respect to soil type and soil constraint changes.
9. Develop a conclusion regarding the effects of spatial variability of soil constraints within a soil type at the sub-field level in regards to the magnitude of mechanical stress that is implemented by machine traffic.

8.2 APPENDIX B

USQ Risk Management Plan

University of Southern Queensland

Generic Risk Management Plan

Workplace (Division/Faculty/Section): FACULTY OF HEALTH, ENGINEERING AND SCIENCES		
Assessment No (if applicable):	Assessment Date: 12/10/2022	Review Date: (5 years maximum) 12/10/2025
Context: What is being assessed? Describe the item, job, process, work arrangement, event etc: ENG4112 Research Project		
Assessment Team – who is conducting the assessment?		
Assessor(s): Student Others consulted: (eg elected health and safety representative, other personnel exposed to risks)		

Step 1 – Identify the hazards (use this table to help identify hazards then list all hazards in the risk table)		
General Work Environment		
☒ Sun exposure	☐ Water (creek, river, beach, dam)	☐ Sound / Noise
☐ Animals / Insects	☐ Storms / Weather/Wind/Lightning	☒ Temperature (heat, cold)
☐ Air Quality	☐ Lighting	☐ Uneven Walking Surface
☐ Trip Hazards	☐ Confined Spaces	☐ Restricted access/egress
☐ Pressure (Diving/Altitude)	☐ Smoke	☐
Other/Details:		
Machinery, Plant and Equipment		
☐ Machinery (fixed plant)	☒ Machinery (portable)	☐ Hand tools
☐ Laser (Class 2 or above)	☐ Elevated work platforms	☐ Traffic Control
☐ Non-powered equipment	☐ Pressure Vessel	☐ Electrical
☐ Vibration	☐ Moving Parts	☐ Acoustic/Noise
☐ Vehicles	☐ Trailers	☐ Hand tools
Other/Details:		
Manual Tasks / Ergonomics		
☐ Manual tasks (repetitive, heavy)	☐ Working at heights	☐ Restricted space
☐ Vibration	☐ Lifting Carrying	☐ Pushing/pulling
☐ Reaching/Overstretching	☐ Repetitive Movement	☐ Bending
☐ Eye strain	☐ Machinery (portable)	☐ Hand tools
Other/Details:		
Biological (e.g. hygiene, disease, infection)		
☐ Human tissue/fluids	☐ Virus / Disease	☐ Food handling
☐ Microbiological	☐ Animal tissue/fluids	☐ Allergenic
Other/Details:		
Chemicals Note: Refer to the label and Safety Data Sheet (SDS) for the classification and management of all chemicals.		
☐ Non-hazardous chemical(s)	☐ 'Hazardous' chemical (Refer to a completed hazardous chemical risk assessment)	
☐ Engineered nanoparticles	☐ Explosives	☐ Gas Cylinders
Name of chemical(s) / Details:		
Critical Incident – resulting in:		
☐ Lockdown	☐ Evacuation	☐ Disruption
☐ Public Image/Adverse Media Issue	☐ Violence	☐ Environmental Issue
Other/Details:		
Radiation		
☐ Ionising radiation	☐ Ultraviolet (UV) radiation	☐ Radio frequency/microwave
☐ Infrared (IR) radiation	☐ Laser (class 2 or above)	☐
Other/Details:		
Energy Systems – incident / issues involving:		
☐ Electricity (incl. Mains and Solar)	☐ LPG Gas	☐ Gas / Pressurised containers
Other/Details:		
Facilities / Built Environment		
☒ Buildings and fixtures	☐ Driveway / Paths	☐ Workshops / Work rooms
☐ Playground equipment	☐ Furniture	☐ Swimming pool
Other/Details:		
People issues		
☐ Students	☐ Staff	☐ Visitors / Others
☐ Physical	☐ Psychological / Stress	☐ Contractors
☐ Fatigue	☐ Workload	☐ Organisational Change
☐ Workplace Violence/Bullying	☐ Inexperienced/new personnel	☐
Other/Details:		

Step 1 (cont)	Step 2	Step 2a	Step 3			Step 4				
Hazards: From step 1 or more if identified	**The Risk:** What can happen if exposed to the hazard with existing controls in place?	**Existing Controls:** What are the existing controls that are already in place?	**Risk Assessment:** (use the Risk Matrix on p3) Consequence x Probability = Risk Level			**Additional controls:** Enter additional controls if required to reduce the risk level	**Risk assessment with additional controls:** (use the Risk Matrix on p3 – has the consequence or probability changed?)			**Controls Implemented? Yes/No**
			Consequence	Probability	Risk Level		Consequence	Probability	Risk Level	
Example										
Working in temperatures over 35º C	Heat stress/heat stroke/exhaustion leading to serious personal injury/death	Regular breaks, chilled water available, loose clothing, fatigue management policy.	catastrophic	possible	high	temporary shade shelters, essential tasks only, close supervision, buddy system	catastrophic	unlikely	mod	Yes
Injury from moving utility vehicle	Physical Injury	Saftey Induction	Minor	Unlikely	Moderate	Ensure that all operators on site are aware of the intended procedures and act accordingly	Minor	Rare	Low	Yes
Burns from oven operating at 105 degrees Celsius	Physical Injury	Safety Induction	Moderate	Unlikely	Moderate	Proceed with caution when moving around the oven, ensure it is cool to touch before loading/ unloading, use gloves	Moderate	Rare	Low	Yes
Conducting experiments in a laboratory environment	Physical Injury	laboratory Induction	Minor	Rare	Low	Wear appropriate PPE, ensure that all laboratory inductions have been completed and supervision is present when required	Minor	Rare	Low	Yes

Step 6 – Approval

Drafter's Comments:

Relatively low risk opertion, implementing additional controls will ensure safe practice.

Drafter Details:

Name: Danny O'Connor Signature: D O'Connor Date: 12/10/2022

Assessment Approval: (Extreme or High = VC, Moderate = Cat 4 delegate or above, Low = Manager/Supervisor)

I am satisfied that the risks are as low as reasonably practicable and that the resources required will be provided.

Name: Guangnan Chen Signature: [redacted] Date: 12/10/2022

Position Title: Associate Professor